[AMERICAN JOURNAL OF SCIENCE, VOL. 294, FEBRUARY, 1994, P. 173–236]

IGNEOUS PETROGENESIS AND TECTONIC SETTING OF THE ELKAHATCHEE QUARTZ DIORITE, ALABAMA APPALACHIANS: IMPLICATIONS FOR PENOBSCOTIAN MAGMATISM IN THE EASTERN BLUE RIDGE

MARK S. DRUMMOND*, DAVID T. ALLISON**, and DAVID J. WESOLOWSKI***

ABSTRACT. The Elkahatchee Quartz Diorite (EQD) is a pre-metamorphic (Penobscot age, 490-500 Ma) batholith and the largest intrusive complex (880 km^2) exposed in the Blue Ridge province of the southern Appalachians. Slightly peraluminous to metaluminous, calc–alkaline I-type tonalite–granodiorite is the principal lithology of the batholithic complex, with subordinate cumulate hornblende–biotite gabbro–diorite and biotite–epidote schistose enclaves, quartz–biotite metadacite porphyry, and felsic granitoids (granite, trondhjemite, and quartz monzonite). These lithologies display a slight normal zonation with accumulation of rare gabbro-diorite enclaves around the outer margin, followed by the dominant tonalite-granodiorite, and a concentration of felsic granitoids in the batholithic core. Schistose enclaves are scattered throughout the EQD as meter- to centimeter-size elliptical bodies. The enclaves are interpreted to represent disrupted fragments of cumulate material that formed as near-liquidus sidewall cyrstallization products. Active convection in the EQD magma chamber segmented the gabbro-diorite enclaves into discrete meter-size enclaves along the batholith's outer margin. Convective transportation of gabbro-diorite cumulate material into the interior of the evolving granitic magma chamber led to mechanical disaggregation, solid-melt reaction, and ultimately schistose enclave generation. Hornblende barometry and hornblende-plagioclase thermometry of the gabbro-diorite enclaves provide crystallization estimates of 1 to 4 kb at 710° to 850°C. Down-plunge structural projection of the map relationships reveals a laccolithic geometry for the EQD. Previously unreported metadacite porphyry occurrences interpreted as being a cogenetic volcanic carapace suggest that the EQD may have experienced emplacement into its own volcanic ejecta. A broad range of SiO_2 (47-74 percent) is represented by the enclaves (<60 percent SiO_2) and granitoids (>60 percent of SiO_2) of the EQD. Based upon least squares mixing calculations, major and minor element covariation is best explained by crystal fractionation. A two-stage crystallization process is invoked to represent the changing proportions of crystalline phases with magma evolution. Modeling of REE, Sr, and O isotopes and other trace element parameters indicates that the parental EQD magma was derived from partial melting of a source consisting of altered MORB plus minor deep sea sediment. Mafic tonalite-granodiorite parental magmas would exist in equilibrium with a restite assemblage of 30 percent hornblende–30 percent

* Department of Geology, University of Alabama at Birmingham, Birmingham, Alabama 35294.
** Department of Geology and Geography, University of South Alabama, Mobile, Alabama 36688.
*** Geochemistry Group, Chemistry Division, Oak Ridge National Laboratory, P.O. Box 2008, Oak Ridge, Tennessee 37831.

garnet–40 percent clinopyroxene (that is, hornblende eclogite). The EQD was probably generated from a subducting slab during Penobscotian orogenesis, underwent dynamic sidewall crystallization upon ascent through mid- to upper-crustal levels, and experienced final emplacement in a subvolcanic regime. We suggest that the EQD represents continental margin magmatism associated with incipient subduction of an oceanic slab beneath Laurentia. This investigation has compiled numerous Penobscot age plutonic, tectonic (ophiolite emplacement), and metamorphic events distributed throughout the Appalachians, which are proximal to previously proposed Laurentian margins (for example, Blue-Green-Long axis and the eastern North American gravity high). We suggest that the Penobscot age orogenesis may have spanned the length of the Appalachians and is, in part, represented by continental margin magmatism, such as the EQD.

INTRODUCTION

The southern Appalachians are a classic orogen in terms of structural complexity, polymetamorphism, and prolonged history of intrusive and extrusive events. Various models of collisional tectonics can be tested relative to the polygenic growth of the southern Appalachian orogen utilizing field and structural observations and seismic studies. Granitoid petrology research has evolved to the stage where specific granite types of different origin can be used to infer different kinds of tectonic settings (Pitcher, 1983, 1987; Pearce, Harris, and Tindle, 1984; Drummond and Defant, 1990; Barbarin, 1990). Each genetic type of granitoid displays distinct field, petrographic, and geochemical characteristics that record valuable information about the mechanism of emplacement, petrogenetic evolution, and source rock composition. These relationships ultimately can reveal a specific tectonic environment associated with the intrusive event, allowing the granitic body to act as an additional informative probe into the lithosphere.

This paper evaluates the dynamic and petrogenetic history of the Elkahatchee Quartz Diorite (EQD), in order to constrain more tightly the tectonic development and crustal evolution of the southern Appalachians. The EQD is a premetamorphic intrusive body of batholithic proportions and represents the largest granitic body (880 km^2) exposed in the Blue Ridge province of the southern Appalachians (fig. 1). Table 1 lists the available geochronologic data on the EQD. The 490 to 500 Ma Rb-Sr whole-rock and U-Pb zircon ages on the EQD have been interpreted as magmatic crystallization ages (Russell, Odom, and Russell, 1987), whereas the Rb-Sr and K-Ar mineral ages were interpreted to represent uplift and cooling ages appropriate for the closure temperature of the mineral isotopic systems. Wedowee and Hatchet Creek Group amphibolite facies metasedimentary rocks are the host rocks to the EQD and are interpreted to represent Eocambrian to mid-Cambrian slope-and-rise turbidite sediments associated with the stabilization of a passive margin (Thomas and others, 1980; Thomas and Neathery, 1980; Drummond, ms; Drummond, Wesolowski, and Allison, 1988).

LITHOLOGIC DESCRIPTION

Slightly peraluminous to metaluminous, calc-alkaline I-type biotite tonalite and granodiorite in roughly equal proportions (fig. 2) are the principal compositional components (approx 90 percent) of the EQD. The tonalites-granodiorites have color indices typically ranging between 15 to 20 (Drummond, ms). Granodiorite and tonalite are represented in roughly equal proportions and display no recognizable distribution pattern. The EQD displays a medium-grained, hypidiomorphic equigranular texture. A majority of mineral grains have subhedral to anhedral crystal shapes and are commonly aligned in a pervasive gneissic fabric (S_1). The gneissic fabric was developed in the EQD during a D_1-M_1 dynamothermal event and is concordant with the dominant foliation in the Wedowee and Hatchet Creek Group host rocks (Drummond, ms; Moore, Tull, and Allison, 1987; Tull, 1987). The D_1-M_1 event affected the entire Northern Alabama Piedmont and is thought to be associated with the Early to Middle Devonian Acadian orogeny on the basis of geochronologic and geologic evidence (Tull, 1978 and 1980).

Subordinate peraluminous biotite-muscovite granite, trondhjemite, and quartz monzonite (fig. 3, Rockford-type granitoids and leucocratic Elkahatchee gneiss) are spatially associated with the EQD; some of these more felsic granitoids (color index <5) may represent differentiates of the tonalite-granodiorite magma. Below we will demonstrate the geochemical compatibility of some of the felsic granitoids with the tonalites-granodiorites of the EQD. Those felsic granitoids considered cogenetic with the tonalites-granodiorites exhibit a strong foliation and lineation (leucocratic Elkahatchee gneiss, fig. 3). The texture of the leucocratic Elkahatchee gneiss is distinct from the fine-grained, weakly foliated trondhjemite dikes and post-tectonic, non-foliated leucogranites that crosscut the EQD. The syngenetic felsic granitoids are sparsely scattered throughout the EQD's main body, but there is a major concentration of strongly lineated, leucocratic Elkahatchee gneiss in the approximate geographic center of the EQD outcrop area (fig. 3).

Three previously unreported quartz-biotite metadacite porphyry occurrences have been found in the central portion and on the outer margin of the EQD (fig. 3), as small localized outcrops. These metadacite lithologies are never found intercalated with the metasedimentary country rocks but are entirely enclosed by the EQD. At one locality, metadacite and EQD are present with foliation penetrating both lithologies, indicating that the metadacite is pre-D_1-M_1 regional metamorphism. A folded 1 m wide vein of EQD intrudes the metadacite. The metadacite and EQD are crosscut by a graphic-textured pegmatite and quartz vein. The metadacite has a porphyritic character with medium-grained plagioclase and biotite phenocrysts set in a light gray matrix composed of fine-grained quartz, plagioclase, and biotite. Alignment of the biotite phenocrysts parallel with F_1 fold axes during D_1-M_1 regional metamorphism created a strong mineral lineation. Plagioclase phenocrysts are either euhedral to subhedral, zoned and exhibit well-developed Carlsbad twins,

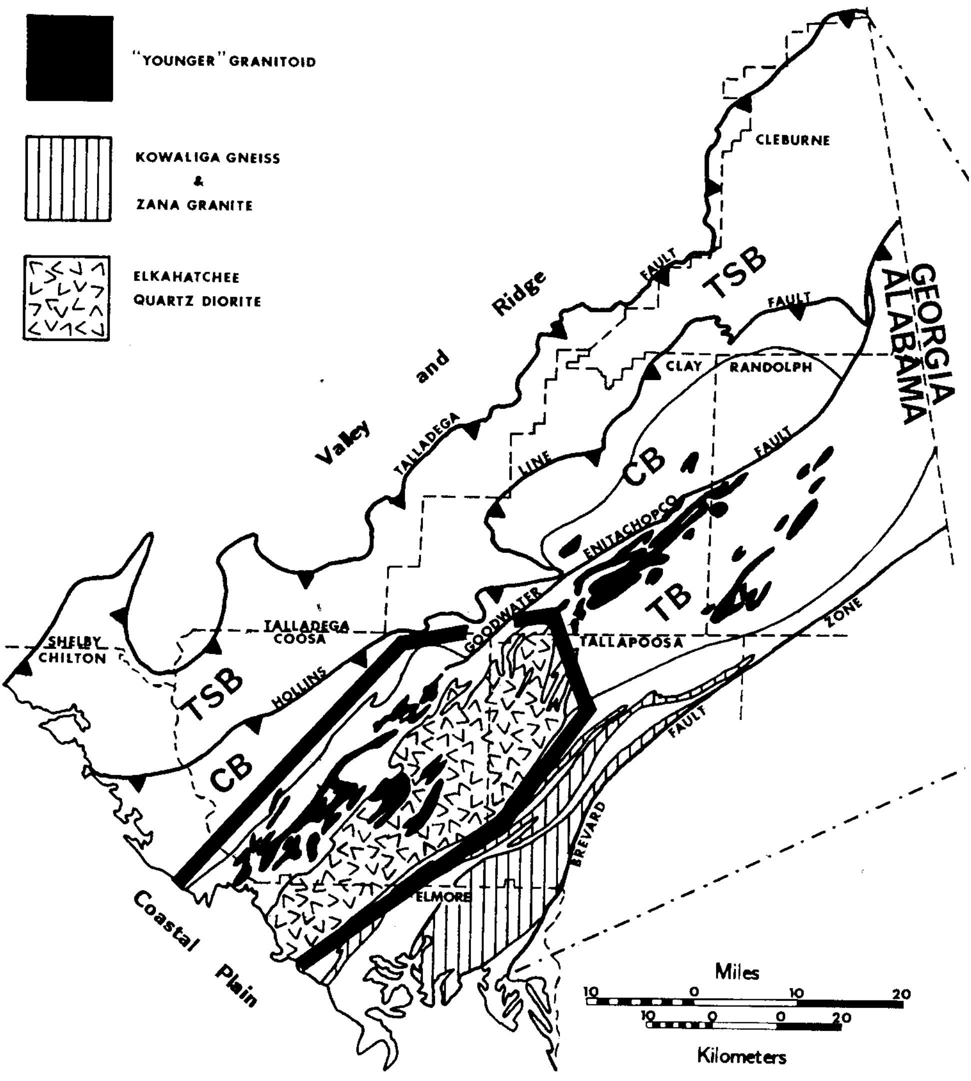
"YOUNGER" GRANITOID
KOWALIGA GNEISS
&
ZANA GRANITE
ELKAHATCHEE
QUARTZ DIORITE
CLEBURNE
FAULT
TSB
GEORGIA
ALABAMA
Valley and Ridge
TALLADEGA
LINE
CLAY
RANDOLPH
CB
ENITACHOPCO
TB
GOODWATER
TALLADEGA
COOSA
TALLAPOOSA
ZONE
SHELBY
CHILTON
HOLLINS
BREVARD
ELMORE
Coastal Plain
Miles
10 0 10 20
10 0 0 20
Kilometers

Figure 1

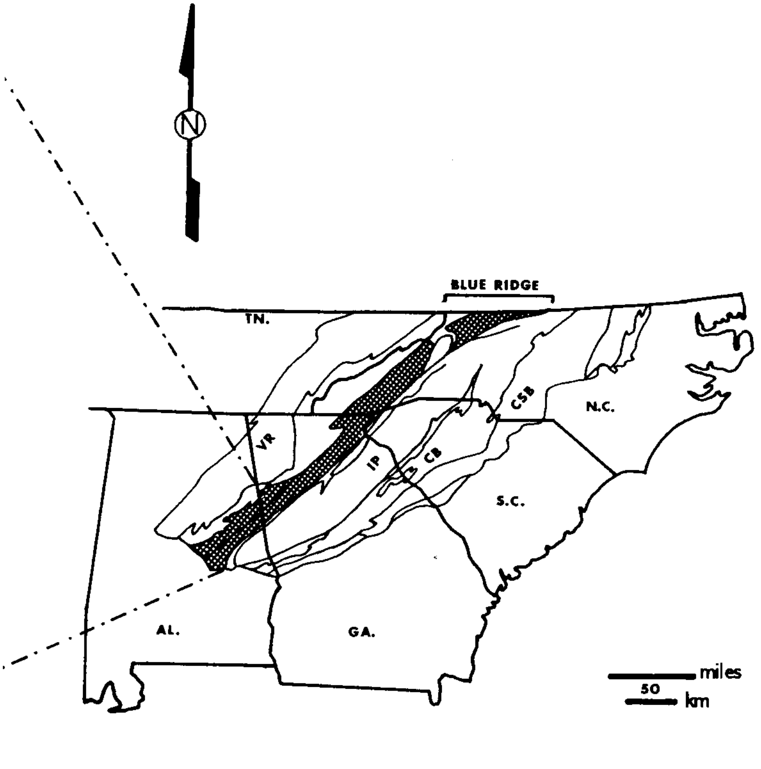

Fig. 1. Generalized geologic map of the Northern Alabama Piedmont with granitoid distribution and lithotectonic subdivision after Tull (1978, 1984, 1987). Study area is outlined and shown in detail in figure 3. Abbreviations: TSB = Talladega Slate Belt/ Talladega block, CB = Coosa block, and TB = Tallapoosa block. Southern Appalachian lithotectonic map after Hatcher and Odom (1980); VR = Valley and Ridge, IP = Inner Piedmont, CB = Charlotte Belt, and CSB = Carolina Slate Belt.

TABLE 1

Isotopic ages and characterization of the EQD

1. Isotopic ages

	Rb-Sr whole-rock	*U-Pb zircon*	*Mineral ages*
Russell (1975)	501 ± 51 Ma ($^{87}Sr/^{86}Sr)_i$ = 0.7036	528 ± 10 Ma	
Russell (ms)	490 ± 13 Ma ($^{87}Sr/^{86}Sr)_i$ = 0.7036	516 Ma	
Russell, Odom, and Russell (1987)	490 ± 28 Ma ($^{87}Sr/^{86}Sr)_i$ = 0.7036	496 ± 14 Ma	
Wampler, Neathery, and Bentley (1970)			328 ± 10 Ma (biotite, K-Ar) 324 ± 10 Ma (musc, K-Ar)
Crawford and Russell (1989)			348 Ma (musc, Rb-Sr)

2. Whole-rock oxygen isotope average = 9.7 ± 0.4 permil (n = 7)
from Drummond (ms) and Wesolowski, Drummond, and Gomolka (1987)

3. Sr isotopic source characterization

Given:	*Sr isotopic character*	*Sr content (ppm)*
MORB average	0.70280 (Faure, 1986)	130 (Brophy and Marsh, 1986)
500 Ma seawater	0.70890 (Faure, 1986)	8 (Henderson, 1982)
Deep-sea sediment	0.7150 (Hole and others, 1984)	1144 (Hole and others, 1984)

Determine: A reasonable mixture of the above three components to derive the $(^{87}Sr/^{86}Sr)_i$ = 0.7036 of the EQD.

0.7036 = 93 percent MORB + 6.3 percent seawater + 0.7 percent sediment (percent by volume).

0.7036 = 93.1 percent MORB + 0.6 percent seawater + 6.3 percent sediment (percent of Sr budget).

or occur as glomeroporphyritic clots. The metadacites are moderately peraluminous (1-2 wt percent normative corundum) and fall within the trondhjemite compositional field (fig. 2). Both the metadacites and trondhjemites from this study are high-Al trondhjemites (Barker and

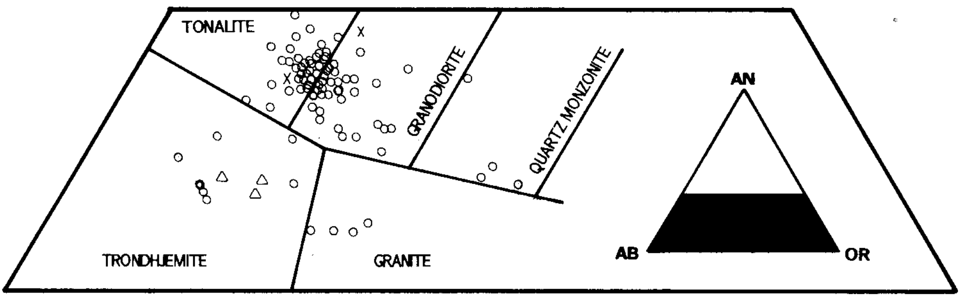

Fig. 2. CIPW normative Ab-An-Or ternary granitic rock classification scheme after Barker (1979). Symbology: Circle = all granitic rocks from this study, triangle = metadacite, X = schistose xenoliths. The data shown here are from this study (representative analyses listed in table 7) or from Drummond (ms).

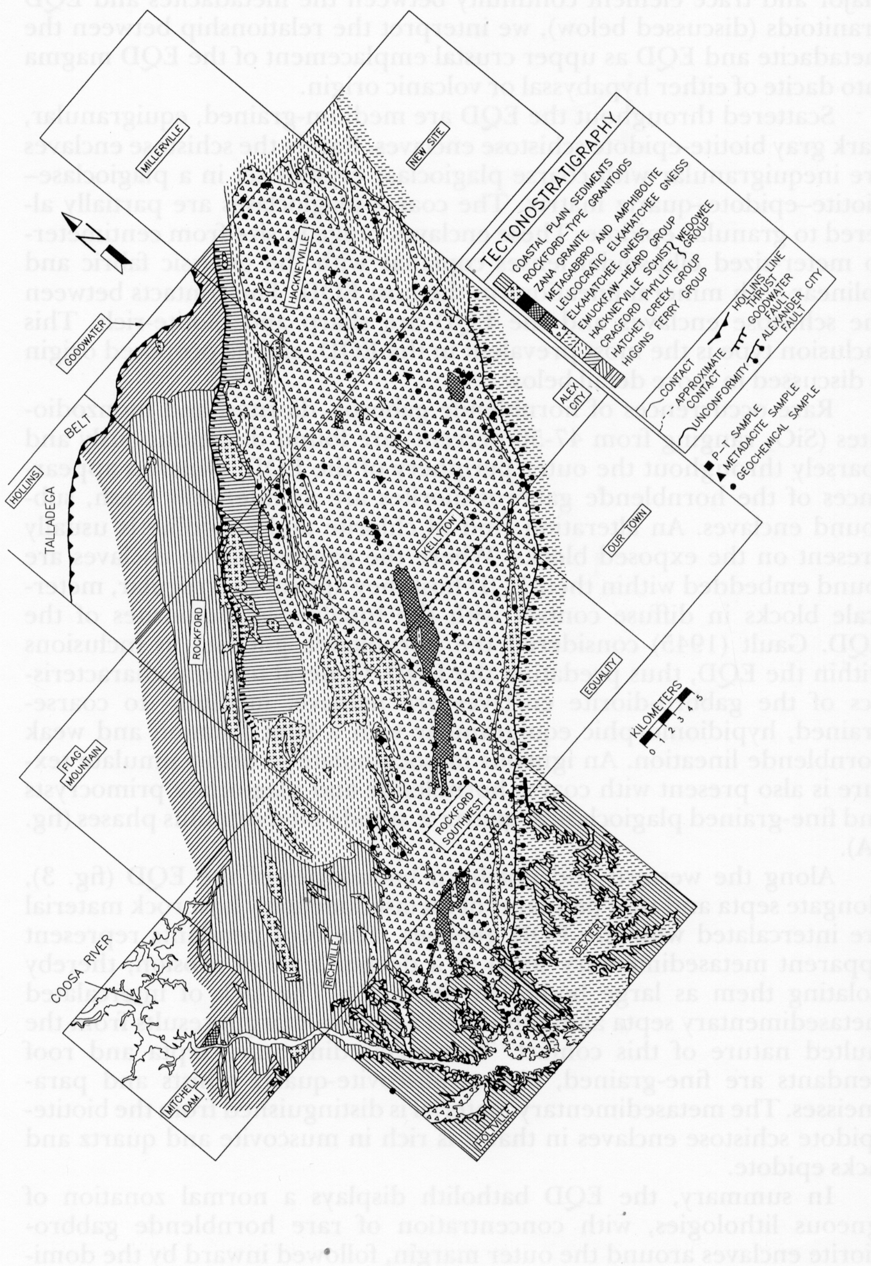

Fig. 3. Geologic map of the EQD complex and metamorphic host rocks. The names to the sixteen $7\frac{1}{2}$ minute quadrangle sheets used in this study are given.

others, 1976). On the basis of the field relationships of the metadacites with the EQD, the mineralogical similarity between the metadacites and the EQD host (that is, early crystallizing plagioclase and biotite), and major and trace element continuity between the metadacites and EQD granitoids (discussed below), we interpret the relationship between the metadacite and EQD as upper crustal emplacement of the EQD magma into dacite of either hypabyssal or volcanic origin.

Scattered throughout the EQD are medium-grained, equigranular, dark gray biotite-epidote schistose enclaves. Rarely the schistose enclaves are inequigranular with coarse plagioclase crystals set in a plagioclase–biotite–epidote–quartz matrix. The coarse plagioclases are partially altered to granular epidote. These enclaves range in size from centimeter- to meter-sized ellipsoidal lenses coplanar with the gneissic fabric and colinear with mineral lineations in the host EQD. The contacts between the schistose enclaves and the EQD are sharp and biotite-rich. This inclusion type is the most prevalent in the EQD, and its proposed origin is discussed in more detail below.

Rare occurrences of hornblende gabbros, diorites, and monzodiorites (SiO_2 ranging from 47-56 percent) are found discontinuously and sparsely throughout the outer periphery of the EQD. Outcrop appearances of the hornblende gabbros-diorites are as internally fresh, subround enclaves. An alteration rind of chlorite and actinolite is usually present on the exposed blocks. Where the gabbro-diorite enclaves are found embedded within their EQD host they appear as irregular, meter-scale blocks in diffuse contact with the tonalites-granodiorites of the EQD. Gault (1945) considered the hornblende gneisses as inclusions within the EQD, thus predating the EQD. General textural characteristics of the gabbro-diorite enclaves are massive, medium- to coarse-grained, hypidiomorphic equigranular with a faint foliation and weak hornblende lineation. An igneous mesocumulate to orthocumulate texture is also present with coarse hornblende and plagioclase primocrysts and fine-grained plagioclase ± quartz ± sulfide intercumulus phases (fig. 4A).

Along the western and northern boundaries of the EQD (fig. 3), elongate septa and roof pendants of metasedimentary host rock material are intercalated with the EQD gneisses. The roof pendants represent apparent metasedimentary septa at a deeper level of erosion, thereby isolating them as large bodies in the EQD. The lack of intercalated metasedimentary septa along the EQD's eastern margin results from the faulted nature of this contact. The metasedimentary septa and roof pendants are fine-grained, biotite-muscovite-quartz schists and paragneisses. The metasedimentary material is distinguished from the biotite-epidote schistose enclaves in that it is rich in muscovite and quartz and lacks epidote.

In summary, the EQD batholith displays a normal zonation of igneous lithologies, with concentration of rare hornblende gabbro-diorite enclaves around the outer margin, followed inward by the domi-

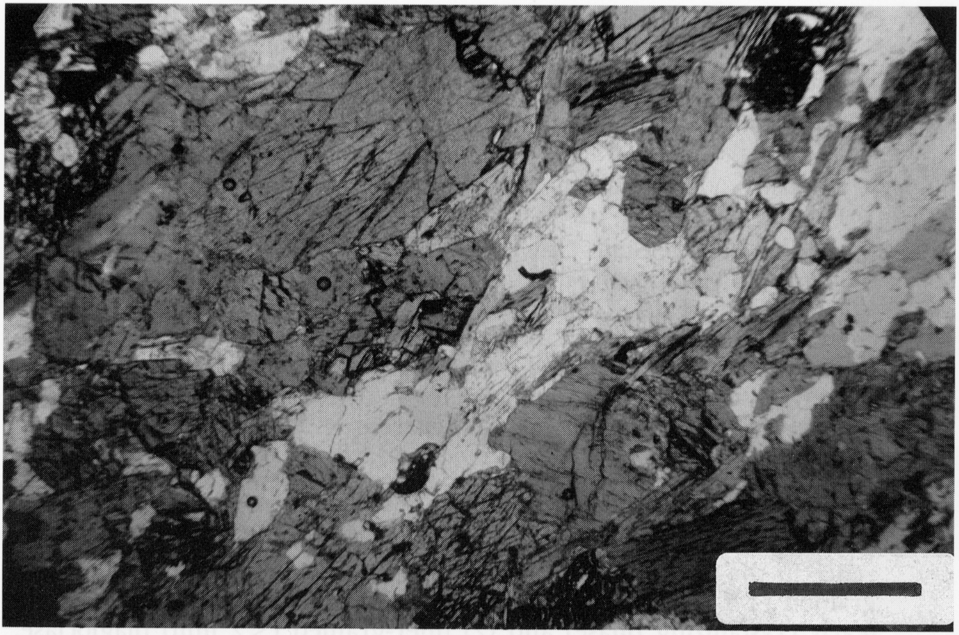

A.

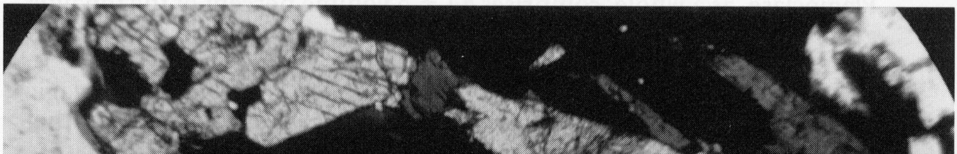

B.

Fig. 4(A) Photomicrograph of biotite-hornblende gabbro enclave (sample E566) exhibiting cumulus hornblende (dark grains) and intercumulus quartz and feldspar. Scale = 1 mm.

(B) Photomicrograph of magmatic epidote textural relations. Sample MD-609, euhedral to subhedral epidote with magmatic biotite. Note the tear-drop shaped allanite core embedded in coarse-grain epidote and associated unaltered biotite (dark grains). Scale = 0.5 mm.

nant tonalite-granodiorite, and a concentration of felsic granitoids in the batholithic core.

MINERALOGY, MINERAL CHEMISTRY, AND CONDITIONS OF CRYSTALLIZATION

Analytical methods.—Microprobe analyses of minerals were performed at Florida State University (50 analyses) and the University of Alabama (150 analyses). Full analytical details and mineral analyses of the EQD performed at FSU are given in Drummond (ms and 1987). Mineral chemistries determined at UA's Central Analytical Facility Electron Microprobe Center were analyzed on a JEOL-8600 Superprobe. Operating conditions at UA were: probe diameter = 20 (feldspar analysis) or 10 (for all other phases) microns, sample current = 20 na, and accelerating voltage = 15 kV. Natural mineral standards were used for elemental calibration. The data reduction scheme of Bence and Albee (1968) was used in this study.

Plagioclase feldspar.—Plagioclase has two common modes of occurrence in the tonalites-granodiorites of the EQD: (1) unaltered, coarse-grained (4-5 mm length), subhedral-euhedral plagioclase primocrysts (early crystallizing phase) and (2) finer-grained (<2 mm) plagioclase. Plagioclase, as a whole, comprises 44 ± 5 volume percent of the tonalites-granodiorites (Drummond, ms) and represents the most abundant phase in these lithologies.

Plagioclase primocrysts can be distinguished from the other plagioclases in the EQD by their distinctly coarser-grained size and by their chemistry. Gault (1945) referred to this population of plagioclase as having a "phenocryst-like" habit. The average composition of the unaltered primocrysts in the tonalites-granodiorites is $An_{34\pm3}$. They are either unzoned, weakly zoned, or display a strong normal zonation (An_{39} core to An_{32} rim). Some primocrysts are poikilitic with euhedral biotite and apatite inclusions. Representative primocryst analyses are listed in table 2.

The finer-grained plagioclase has an average composition of $An_{24\pm2}$ (see table 2 for representative analyses) and is usually in mutual contact with perthite + microcline + myrmekite. It is always anhedral, unzoned, unaltered, and interstitial to the coarser-grained primocrysts. Both the finer-grained plagioclase and myrmekite ($An_{24\pm5}$ avg) may represent late stage, exsolution phases from alkali feldspar due to their fine-grained, interstitial habit and ubiquitous association with K-feldspar.

Primocryst ($An_{35\pm3}$ avg) and fine-grained plagioclase in hornblende diorite-monzodiorite enclaves (E40 and E204, respectively; table 2) are chemically (table 2) and petrographically similar to plagioclase from the tonalites-granodiorites. These similarities are consistent with the cumulate interpretation for the dioritic rocks, as presented below. Plagioclases from hornblende gabbro enclaves in the EQD complex are strongly zoned and more calcic ($An_{48\pm3}$ core, $An_{32\pm9}$ rim; table 2) than those in the dioritic and tonalitic lithologies.

TABLE 2

Representative feldspar analyses

Sample	E40	E40	E204	E204	E566	E566	E536	E536	MD609	MD609	E40	E40	MD289	E204	E204	E536
Mineral*	ppc	ppr	ppc	ppr	ppc	ppr	ppc	ppr	ppc	ppc	pgc	pgr	pgc	kfc	kfr	kfc
SiO_2	57.24	57.90	58.45	58.67	53.98	57.28	58.59	58.91	58.76	59.56	58.87	60.52	60.51	64.16	63.71	62.33
Al_2O_3	27.28	26.18	26.67	25.64	29.00	27.14	25.89	25.80	26.56	26.17	24.93	24.78	24.33	19.27	18.86	19.30
CaO	7.83	6.95	7.54	6.79	10.67	7.63	6.73	6.67	7.22	6.63	5.71	5.14	5.60	0.05	0.05	0.00
Na_2O	7.51	7.97	7.42	7.74	5.52	7.00	7.82	8.05	7.62	7.98	8.70	9.12	8.60	0.77	0.81	1.14
K_2O	0.03	0.07	0.12	0.06	0.05	0.15	0.20	0.19	0.11	0.10	0.19	0.09	0.12	15.75	15.83	14.92
Total	99.90	99.07	100.19	98.91	99.22	99.21	99.23	99.61	100.28	100.44	98.39	99.65	99.16	100.00	98.71	97.70
							- based on 8 oxygens -									
Si	2.567	2.612	2.606	2.644	2.453	2.580	2.635	2.640	2.616	2.643	2.669	2.701	2.713	2.963	2.962	2.943
Al	1.442	1.392	1.401	1.362	1.553	1.441	1.372	1.362	1.394	1.369	1.332	1.304	1.285	1.049	1.042	1.074
Sum Z	4.009	4.004	4.007	4.006	4.006	4.021	4.007	4.002	4.010	4.012	4.001	4.005	3.998	4.012	4.004	4.017
Ca	0.376	0.336	0.360	0.328	0.520	0.368	0.325	0.320	0.344	0.315	0.277	0.246	0.269	0.002	0.002	0.000
Na	0.653	0.697	0.642	0.676	0.486	0.611	0.682	0.699	0.658	0.687	0.764	0.789	0.748	0.069	0.074	0.104
K	0.002	0.004	0.006	0.004	0.003	0.009	0.012	0.011	0.006	0.006	0.011	0.005	0.007	0.928	0.947	0.899
Sum X	1.031	1.037	1.008	1.008	1.009	0.988	1.019	1.029	1.008	1.008	1.052	1.040	1.024	0.999	1.023	1.003
TOTAL	5.040	5.041	5.015	5.014	5.015	5.009	5.026	5.031	5.018	5.020	5.053	5.045	5.022	5.011	5.027	5.020
mol% An	36.5	32.4	35.7	32.5	51.5	37.2	31.9	31.1	34.1	31.3	26.4	23.6	26.3	0.2	0.2	0.0
mol% Ab	63.3	67.2	63.7	67.1	48.2	61.8	66.9	67.9	65.3	68.1	72.6	75.9	73.1	6.9	7.2	10.4
mol% Or	0.2	0.4	0.6	0.4	0.3	1.0	1.2	1.0	0.6	0.6	1.0	0.5	0.6	92.9	92.6	89.6

* ppc and ppr = primocryst plagioclase core and rim, respectively, pgc and pgr = groundmass plagioclase core and rim, respectively, kfc and kfr = K-feldspar core and rim, respectively.

K-feldspar.—K-feldspar is found both as perthite (string and patch varieties) and microcline (table 2). In the tonalites-granodiorites, K-feldspar is commonly finer-grained (<1 mm) than the other major phases and occurs as interstitial, anhedral grains. Modal abundances of K-feldspar in the tonalite-granodiorites range from trace amounts to 5 volume percent, with perthite being the most common variety. K-feldspar in the dioritic enclaves increases in abundance in the monzodioritic varieties, where relatively coarse (2-3 mm) perthite of average composition $Ab_{7\pm1}$ occurs (table 2). Perthite–microcline–myrmekite–quartz microveins and intergranular patches in the granodiorites-tonalites are taken to represent the last residual melt phase in the granitoid prior to complete solidification.

Biotite.—Biotite is the dominant ferromagnesian phase in the tonalites-granodiorites of the EQD comprising 16 ± 3 volume percent. The length of individual biotite grains commonly ranges from 1 to 2 mm. Biotite is pleochroic from pale straw to foxy red-brown or dark chocolate brown and usually exhibits a slight undulatory extinction. Biotite and interlayered secondary muscovite commonly wrap plagioclase primocryst augen in the S_1 foliation fabric outlining the plagioclase morphology. Representative biotite analyses are listed in table 3. Tonalite-granodiorite biotites (E536, MD609, MD289) are more siderophyllite-rich than those coexisting with hornblende in the dioritic enclaves (E40 and E204).

Hornblende.—Hornblende in the EQD is restricted to those gabbro-diorite enclaves with SiO_2 contents between 47 to 56 percent. The hornblendes are stumpy, prismatic, subhedral-euhedral crystals, medium-grained (2-5 mm length), and greenish black in color. Their pleochroic scheme is X = yellow green, Y = light yellow, and Z = green. Hornblende displays either a mesocumulate texture with interstitial plagioclase and quartz in the gabbros (fig. 4A) or an orthocumulate texture with equal proportions of cumulate plagioclase primocrysts in the dioritic enclaves. In the dioritic enclaves, hornblende can be found as inclusions within plagioclase primocrysts, and euhedral sphene occurs as inclusions in the hornblende. Rare occurrences of zircon inclusions with pleochroic halos in the hornblende have been reported (Gault, 1945) but have not been observed in this study. Representative hornblende analyses from the EQD complex are listed in table 4.

Hornblende is commonly found with a biotite + Fe-epidote replacement assemblage. In a study of magmatic epidote-bearing granodiorites and tonalites of northwestern North America, Zen and Hammarstrom (1984) found that hornblende was resorbed and replaced by Fe-epidote following reaction (1), below, where hornblende (HB), plagioclase (AN), epidote (EP), and biotite (BT) are solid phases, and alkali feldspar (af), magnetite (mt), and quartz (q) are probably melt components.

$$2\ \mathrm{HB} + 2\ \mathrm{af} + 2\ \mathrm{AN} + 1\ \mathrm{mt} + n\mathrm{H_2O} + m\mathrm{O_2} = 3\ \mathrm{EP} + 3\ \mathrm{BT} + 6\ \mathrm{q} \quad (1)$$

This reaction is associated with increasing f_{H_2O}, f_{O_2}, and activity of alkali feldspar component in the melt that accompanies magmatic differentia-

TABLE 3

Representative biotite analyses

Sample	E40	E40	E204	E204	E566	E566	E715B	E536	E536	MD609	MD609	MD289
Mineral	core	rim	core	rim	core	rim	core	core	rim	core	rim	core
SiO_2	37.63	37.96	38.07	38.21	38.53	38.37	36.96	36.18	36.73	36.99	37.46	35.74
Al_2O_3	15.55	15.78	16.97	17.15	18.37	18.58	17.73	17.30	17.80	16.96	17.34	16.68
TiO_2	1.95	1.97	1.27	1.23	1.18	1.28	2.07	3.15	2.87	2.53	2.10	1.70
FeO	14.29	14.25	16.53	16.18	11.11	11.60	17.87	20.51	20.83	19.02	17.91	21.77
MnO	0.14	0.18	0.28	0.29	0.01	0.13	0.34	0.39	0.34	0.33	0.31	0.43
MgO	15.14	15.12	13.68	13.52	17.07	16.51	10.70	8.89	9.19	11.15	11.66	9.63
K_2O	9.49	9.73	9.59	9.60	9.28	9.37	9.38	9.29	9.27	9.46	9.31	9.04
Total	94.19	94.98	96.38	96.18	95.55	95.83	95.05	95.71	97.02	96.44	96.08	94.99
					- based on 22 oxygens -							
Si	5.656	5.658	5.635	5.656	5.577	5.557	5.586	5.514	5.513	5.551	5.595	5.528
Al^{IV}	2.344	2.342	2.365	2.344	2.423	2.443	2.414	2.486	2.487	2.449	2.405	2.472
Sum Z	8.000	8.000	8.000	8.000	8.000	8.000	8.000	8.000	8.000	8.000	8.000	8.000
Al^{VI}	0.410	0.431	0.595	0.648	0.711	0.729	0.745	0.622	0.662	0.550	0.647	0.569
Ti	0.220	0.221	0.141	0.137	0.128	0.139	0.236	0.361	0.324	0.286	0.236	0.198
Fe^{+2}	1.796	1.776	2.046	2.003	1.344	1.404	2.260	2.613	2.614	2.386	2.237	2.816
Mn	0.018	0.022	0.035	0.036	0.002	0.015	0.044	0.050	0.043	0.042	0.039	0.056
Mg	3.392	3.359	3.020	2.983	3.684	3.565	2.411	2.020	2.057	2.495	2.596	2.222
Sum X,Y	5.836	5.809	5.837	5.807	5.869	5.852	5.696	5.666	5.700	5.759	5.755	5.861
K	1.820	1.849	1.811	1.812	1.715	1.731	1.807	1.807	1.775	1.810	1.774	1.785
TOTAL	15.656	15.658	15.648	15.619	15.584	15.583	15.503	15.473	15.475	15.569	15.529	15.646
mol% phg	58	58	52	51	63	61	42	36	36	43	45	38
mol% sid	23	23	30	31	26	28	41	45	46	37	37	42
mol% ann	19	19	18	18	11	11	17	19	18	20	18	20

Endmember biotite components are defined according to Gunow, Ludington, and Munoz (1980), where: mol percent phlogopite (phg) = (Mg/Sum X,Y) * 100, mol percent siderophyllite (sid) = [((3-Si/Al)/1.75)(1-X_{phg})] * 100, mol percent annite (ann) = (1 − (X_{phg} + X_{sid})) * 100.

TABLE 4

Representative hornblende analyses

Sample	E40	E40	E40	E40	E204	E204	E204	E204	E566	E566
Mineral*	mhc	mhr	mhc	mhr	ahc	ahr	actc	actr	mhc	mhr
SiO_2	48.24	48.01	46.86	47.62	51.13	49.11	52.71	52.75	47.79	47.29
Al_2O_3	8.25	8.01	9.44	9.56	5.94	5.68	3.42	3.51	11.83	11.91
TiO_2	0.40	0.39	0.74	0.74	0.56	0.52	0.12	0.09	0.64	0.50
FeO	12.25	12.27	13.14	13.44	13.02	13.41	11.58	11.48	9.84	9.54
MnO	0.19	0.21	0.20	0.20	0.32	0.31	0.35	0.35	0.18	0.21
MgO	14.13	14.27	13.23	13.41	14.76	14.27	15.44	15.57	14.72	14.09
CaO	12.39	12.13	11.98	12.20	12.59	12.20	12.69	12.66	11.57	11.56
Na_2O	0.94	0.89	1.10	1.11	0.64	0.71	0.33	0.36	1.38	1.31
K_2O	0.23	0.25	0.59	0.48	0.29	0.22	0.02	0.00	0.00	0.00
Total	97.02	96.43	97.28	98.76	99.25	96.43	96.66	96.77	97.95	96.41
					- based on 23 oxygens -					
Si	7.046	7.056	6.879	6.884	7.302	7.255	7.645	7.637	6.805	6.832
Al^{IV}	0.954	0.944	1.121	1.116	0.698	0.745	0.355	0.363	1.195	1.168
Sum T	8.000	8.000	8.000	8.000	8.000	8.000	8.000	8.000	8.000	8.000
Al^{VI}	0.467	0.444	0.513	0.514	0.302	0.245	0.230	0.236	0.792	0.861
Ti	0.044	0.043	0.082	0.080	0.060	0.057	0.013	0.010	0.069	0.054
Mg	3.076	3.126	2.894	2.889	3.142	3.142	3.338	3.360	3.124	3.034
Fe^{+2}	1.413	1.387	1.511	1.517	1.496	1.556	1.405	1.390	1.015	1.051
Mn	0.000	0.000	0.000	0.000	0.000	0.000	0.014	0.004	0.000	0.000
Sum M_1-M_3	5.000	5.000	5.000	5.000	5.000	5.000	5.000	5.000	5.000	5.000
Fe^{+2}	0.083	0.121	0.102	0.108	0.058	0.101	0.000	0.000	0.157	0.102
Mn	0.024	0.026	0.025	0.024	0.039	0.039	0.029	0.039	0.022	0.026
Ca	1.893	1.853	1.873	1.868	1.903	1.860	1.971	1.961	1.765	1.789
Na	0.000	0.000	0.000	0.000	0.000	0.000	0.000	0.000	0.056	0.083
Sum M_4	2.000	2.000	2.000	2.000	2.000	2.000	2.000	2.000	2.000	2.000
Ca	0.046	0.058	0.012	0.022	0.024	0.071	0.001	0.003	0.000	0.000
Na	0.266	0.254	0.313	0.311	0.177	0.203	0.093	0.101	0.325	0.284
K	0.043	0.047	0.110	0.089	0.053	0.041	0.004	0.000	0.000	0.000
Sum A	0.355	0.359	0.435	0.422	0.254	0.315	0.098	0.104	0.325	0.284
TOTAL	15.355	15.358	15.435	15.422	15.254	15.316	15.098	15.104	15.325	15.284
mg#**	0.673	0.675	0.642	0.640	0.669	0.655	0.704	0.708	0.727	0.725

* mhc and mhr = magnesio-hornblende core and rim, respectively, ahc and ahr = actinolitic-hornblende core and rim, respectively, actc and actr = actinolite core and rim, respectively.

** mg# = Mg/(Mg + Fe).

tion. The early crystallization of hornblende suggests that the parental EQD magma contained at least 3.0 wt percent water (Burnham, 1979).

Figure 5 indicates the diversity of hornblende compositions from the three EQD samples analyzed. All the hornblendes are calcic amphiboles

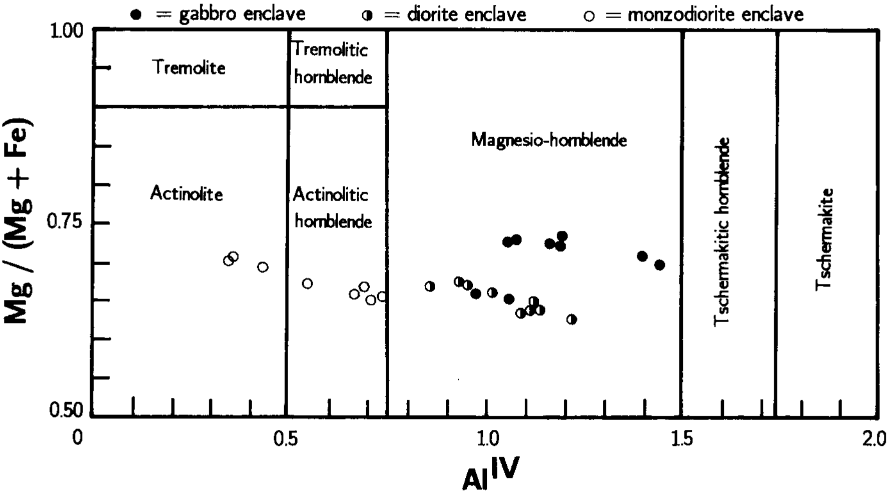

Fig. 5. Hornblende classification diagram for the EQD modified after Leake (1978) and Hammarstrom and Zen (1986).

with two of the samples plotting in the magnesio-hornblende field and the third sample ranging from actinolitic hornblende to actinolite. The biotite-hornblende gabbro enclave (E566) has slightly higher Mg/(Mg + Fe) values relative to the hornblende-biotite diorite enclave (E40). Hornblendes from the monzodiorite (E204) are ragged, anhedral crystals with primary actinolitic hornblende compositions in unaltered crystals. Actinolite in the monzodiorite is a product of deuteric alteration of either actinolitic hornblende rims or near-complete replacement of rare clinopyroxene. The gradation in composition from relatively high Mg# magnesio-hornblende in the gabbro through intermediate Mg# magnesio-hornblende in the diorite to actinolitic hornblende in the monzodiorite may record the continual chemical change with magmatic differentiation. A similar compositional gradation has been reported in the gabbro–diorite–tonalite–granodiorite suites from the Peruvian Andes (Mason, 1985).

Quartz.—Quartz makes up approx 28 volume percent of the EQD's tonalites-granodiorites (Drummond, ms) and varies widely in size from 0.2 to 2.5 mm in diameter. It is generally anhedral in shape and exhibits a highly undulose extinction due to kinematic effects. Quartz is segregated into ribbons of interlocking grains with sutured grain boundaries in localized shear zones.

Accessory minerals.—Apatite, zircon, sphene, magnetite, ilmenite, pyrite, molybdenite, clinopyroxene, and epidote represent the magmatic accessory phase assemblage in the EQD complex. Apatite is always observed to be in mutual contact with or included in biotite. Individual apatite crystals exhibit a short prismatic, euhedral shape and range in size from 0.04 to 1.0 mm in length. One homogeneous population of zircons consists of elongated prismatic, euhedral crystals approx 20 to 40 microns in length. Zircon is always enclosed by coarser-grained phases, such as plagioclase or biotite. Pleochroic halos are developed around zircons that are included in biotite. Primary sphene occurs as discrete brown euhedral crystals that range up to 3 mm in diameter. Inclusions of sphene in biotite and hornblende are common. Sphene analyses (table 5) indicate that coarse sphene phenocrysts are depleted in Fe^{3+} and enriched in Al^{VI} relative to sphenes accompanying the hornblende to biotite reaction. Pyrite and very rare molybdenite represent the only sulfide phases observed in the EQD and occur as discrete, intergranular, an- to subhedral grains.

Clinopyroxene (ferroan diopside, $Wo_{50}En_{35}Fs_{15}$; pyroxene classification scheme of Rock, 1990) occurs in the monzodiorite enclave (E204). Actinolitic rims surround the clinopyroxene resulting from incomplete late- to post-magmatic deuteric alteration. Rare pyroxene is also present in the gabbroic samples but is subordinate to hornblende and biotite. No pyroxene is present in the tonalite-granodiorite samples.

Fe-epidote with pistacite (Ps) contents between Ps_{20} and Ps_{30} is found in the EQD (table 5). A magmatic origin is indicated for the Fe-epidote on the basis of textural criteria outlined by Zen and Hammarstrom (1984) for magmatic epidote, such as eu- to subhedral habit, size similarity between Fe-epidote (0.5-2.0 mm diam) and obvious magmatic phases (hornblende, biotite, plagioclase), straight grain boundaries with hornblende and biotite, Fe-epidote cored by euhedral, yellow-brown allanite, and zoned and twinned crystals (fig. 4B). In fact, allanite and Fe-epidote are considered early-crystallizing phases in the EQD (table 6), with the latter phase playing a key role in the early geochemical differentiation of the EQD (as discussed below). Allanite and Fe-epidote are present in a restricted lithologic (diorite to tonalite) and geochemical (56-64 percent SiO_2) group of the EQD complex, which is consistent with their interpreted early to intermediate stage of crystallization. If the Fe-epidote was subsolidus/metamorphic, we would expect it to be distributed throughout the EQD, such as the secondary Al-rich epidote discussed below, and not restricted to a certain lithologic group. Experimental (Naney, 1983) and petrologic studies (Zen and Hammarstrom, 1984; Evans and Vance, 1987; Barth, 1990; Vyhnal, McSween, and Speer, 1991) have found that Fe-epidote with primary magmatic textural features ranges in composition between Ps_{21} to Ps_{33}. Minor (<10 modal percent) secondary mineralization found throughout the EQD complex is represented by muscovite, Al-rich epidote, chlorite, finely disseminated sphene, ilmenite, and goethite.

Mineral paragenesis.—A general crystallization sequence can be inferred from mineral inclusion and crosscutting relationships in thin section. The order of crystallization is listed in table 6. The relatively early crystallization of zircon, apatite, sphene, and allanite indicates initial

TABLE 5

Representative epidote and sphene analyses

Sample	E40	E40	E204	E204	MD609	MD609	MD224	MD301	E204	E204	E204
Mineral*	pec	per	pec	per	pec	per	pec	sec	spc	spr	psc
SiO_2	37.59	37.03	38.69	38.69	37.03	37.65	37.80	39.08	32.02	30.32	31.57
Al_2O_3	24.60	23.59	26.78	27.11	25.11	26.57	22.80	28.65	1.43	1.48	1.23
TiO_2	0.18	0.21	0.14	0.12	0.24	0.13	0.08	0.16	36.83	36.25	34.65
FeO	9.40	11.13	9.27	9.51	11.10	10.03	13.59	6.19	0.67	0.63	1.66
MnO	0.18	0.37	0.24	0.29	0.33	0.45	0.14	0.18	0.19	0.19	0.31
CaO	23.25	22.57	23.80	23.23	22.67	23.09	23.05	22.86	28.23	27.82	27.83
Total	95.20	94.91	98.92	98.94	96.48	97.91	97.46	97.12	99.36	96.70	97.24
			- based on 12.5 oxygens -						- based on 4 silicons -		
Si	3.094	3.089	3.053	3.050	3.032	3.018	3.105	3.075	4.000	4.000	4.000
Al^{VI}	2.386	2.319	2.491	2.519	2.423	2.509	2.206	2.656	0.210	0.230	0.183
Ti	0.011	0.013	0.008	0.007	0.015	0.008	0.005	0.009	3.459	3.596	3.301
Fe^{+3}**	0.647	0.776	0.612	0.608	0.760	0.672	0.933	0.347	0.094	0.069	0.176
Sum Y	3.044	3.108	3.111	3.144	3.198	3.189	3.144	3.012	3.763	3.895	3.660
Fe^{+2}	0.000	0.000	0.000	0.019	0.000	0.000	0.000	0.060	0.000	0.000	0.000
Mn	0.012	0.026	0.016	0.019	0.023	0.030	0.010	0.013	0.020	0.022	0.033
Ca	2.051	2.017	2.012	1.962	1.988	1.982	2.028	1.927	3.780	3.932	3.777
Sum X	2.067	2.043	2.028	2.000	2.011	2.012	2.038	2.000	3.800	3.954	3.810
TOTAL	8.205	8.240	8.192	8.194	8.241	8.219	8.287	8.087	11.563	11.827	11.470
mol% ps**	21	25	20	20	24	21	30	12			

* pec and per = primary epidote core and rim, respectively, sec = secondary epidote core, spc and spr = sphene primocryst core and rim, respectively, psc = peritectic sphene core associated with the reaction of hornblende to biotite.

** Fe^{+3} partitioned according to stoichiometry. mol percent pistacite (ps) = $Fe^{+3}/(Fe^{+3} + Al^{VI})$.

TABLE 6

Mineral paragenesis of the EQD

Clinopyroxene
Hornblende (non-poikilitic)
Zircon → Apatite → Sphene
Hornblende + **Biotite + Allanite**
Biotite + **Fe-epidote + Andesine "primocrysts"**
Biotite + Fe-epidote + **Andesine + Quartz**
Oligoclase + Quartz + Perthite
(Late stage magmatic to subsolidus)
Clinozoisite + Myrmekite + Microcline + Muscovite + Quartz

Note: Minerals indicated by bold lettering are the dominant phases for the respective paragenetic stage.

saturation of the melt in these phases. The early crystallization or restite behavior of these phases and their low solubility in granitic melts are well documented (Miller and Mittlefehldt, 1982; Gromet and Silver, 1983; Watson and Harrison, 1984).

The rarity of clinopyroxene and hornblende in the EQD may be due to resorption and reaction to biotite and Fe-epidote with decreasing temperature and increasing P_{H_2O} with differentiation. The maximum thermal stability of clinopyroxene in equilibrium with I-type, dacitic melts (1050°C; Rushmer, Holloway, and Wyborn, 1985) and the limited saturation level of ferromagnesian oxides in felsic melts (max 2.5 wt percent FeO + MgO at 1050°C, 8 kb, and 2-5 wt percent H_2O; Miller, Watson, and Rapp, 1985) relative to the ferromagnesian content in the tonalites-granodiorites of the EQD (5.41 wt percent FeO* + MgO avg, n = 70) suggest that the presence of mafic silicate restite or cumulate phases in an I-type granitoid, such as the EQD, is very likely.

Pressure and temperature estimates.—The hornblende diorite and gabbro enclaves of the EQD contain the assemblage quartz + plagioclase + K-feldspar + hornblende + biotite + sphene + Fe-Ti oxide that is required for hornblende barometric estimates. The hornblende barometer is based on the pressure sensitivity of total Al content in hornblende, where Al content increases with pressure. Hornblende crystallization pressures for the EQD have been calculated using the calibration of Johnson and Rutherford (1989). A geothermometer has been devised (Blundy and Holland, 1990) based on the Al^{IV} content of hornblende coexisting with plagioclase in silica-saturated rocks. The reported uncertainty associated with the geobarometer and geothermometer are 0.5 kb and 75°C, respectively. The three EQD samples used in the hornblende-plagioclase thermometry are quartz-bearing and contain hornblende and plagioclase in textural equilibrium. Leake (1971) established two criteria to distinguish igneous amphiboles from altered or metamorphic amphiboles: Si atom < 7.25 per 13eCNK (13 cations minus Ca, Na, and K) and $Al^{VI} < 0.6Al^{IV} + 0.25$ for igneous amphiboles. Only those hornblendes that satisfied the igneous criteria were utilized for P-T determinations.

The gabbroic enclave (E566) recorded the highest average calculated pressure and temperature of 4.30 ± 0.61 kb and 844° ± 25°C. The measure of dispersion about the reported mean temperature and pressure is represented by a one sigma standard deviation from replicate P-T determinations in a single sample. A slightly lower P-T average of 3.06 ± 0.62 kb and 789° ± 30°C was calculated for the diorite enclave (E40). The monzodiorite enclave (E204) recorded the lowest temperature (713° ± 5°C) and pressure (0.88 ± 0.24 kb) of the hornblende-bearing specimens. The low pressure of the monzodiorite is below the calibration range (2-8 kb) for the Johnson and Rutherford (1989) barometer, and its reliability is uncertain.

The following four lines of evidence argue that the EQD's hornblendes have retained an igneous chemistry and that the calculated pressures and temperatures estimate changing magmatic conditions. (1) As pointed out by Hammarstrom and Zen (1986), the use of relatively immobile Al concentrations as the primary criteria for Al-in-hornblende barometry severely retards subsolidus reequilibration of this geobarometer. (2) The average P-T estimates for the Wedowee and Hatchet Creek Group host rocks are 600°C-5.5 kb and 650°C-5.5 kb, respectively (Drummond, ms). The P-T estimates from the metasedimentary host rocks are quite different from the 710° to 850°C and 1 to 4 kb conditions recorded by the EQD, which suggest that metamorphic reequilibration may not have been important in the EQD magmatic mineral assemblage. (3) Average plagioclase compositions from the Wedowee and Hatchet Creek metasedimentary host rocks (Drummond, ms) are oligoclase ($An_{22\pm3}$; mean ± one sigma standard deviation, n = 22), which is distinct from the magmatic andesine ($An_{34\pm3}$) from the EQD. Comparison between hornblende in the EQD and host metamorphic rocks cannot be made due to lack of hornblende in the surrounding metasedimentary rocks. However, as discussed above, only those hornblendes that met Leake's (1971) chemical criteria for igneous hornblende were used in the P-T estimates. (4) The hornblendes used in the P-T calculations exhibited no petrographic evidence of alteration. The hornblende-bearing enclaves have retained an interpreted igneous cumulate texture (fig. 4A) and exhibit little to no metamorphic fabric development.

Therefore, the gabbro–diorite–monzodiorite enclaves are interpreted to have crystallized at different temperatures and pressures, representing accumulation of early crystallizing phases during different stages of an ascending batholith. The gabbro enclave represents the least differentiated cumulate with the earliest crystallizing mineral assemblage, followed by the diorite enclave, and finally the most differentiated monzodiorite enclave. The gabbro to monzodiorite enclaves record a decrease in P-T conditions, which may be due to concomitant ascent, cooling, and geochemical differentiation of the magma chamber.

STRUCTURAL HISTORY

We have completed a comprehensive mapping project on all or parts of sixteen 7.5 min quadrangles from the southern half of the Northern Alabama Piedmont's Ashland-Wedowee belt (fig. 3). On a regional lithotectonic scale, the area mapped represents the extreme southwest exposed portion of the eastern Blue Ridge province of the southern Appalachians. Mapping of approx 1550 km^2 has involved collection of structural data from over 2400 stations. The EQD occurs in the central segment of the map area, and the following discussion addresses the geometry, contact relationships, structural interpretation, and emplacement mechanism of the batholith. A detailed quantitative structural analysis of the study area is beyond the scope of this study and will be covered by Allison and Drummond (in preparation); although the following discussion provides a basic summary of the complex structures present in the study area.

Batholith geometry and contact relationships.—The premetamorphic EQD is a sill-like gneissic body of batholithic proportions (880 km^2). The EQD batholith was intruded into a late Precambrian (?) to early Paleozoic sequence of metasedimentary and metavolcanic lithologies. Contacts between the EQD and the various country rocks are knife-sharp, with an intrusive character demonstrated by incorporated xenolithic material and regional crosscutting of stratigraphic units in the southwest portion of the study area (fig. 3). There is no evidence of contact metamorphism associated with the EQD, nor is there any metamorphic aureole associated with the EQD and the younger intrusive granitoids. If a contact aureole existed around the border of the batholith, it is completely overprinted by the Acadian regional dynamothermal event.

The EQD is concordant to county rock metasediments in most exposures. This relationship is also true on a megascopic scale in the northern portion of the study area; however, the EQD batholith cuts downward through the Hatchet Creek Group stratigraphy in the southern portion of the study area in the Richville and Rockford southwest quadrangles (fig. 3). This discordance represents approx 6 km of structural thickness of country rock. The overall geometry of the EQD conforms to that of a mushroom-shaped (laccolithic) body conformable at the top, which merges into a structurally lower feeder dike portion (fig. 6). The current erosional level has obliquely dissected the intrusive structure, exposing different levels of the batholith over a regional extent. A downplunge projection of the map relationships has been constructed (not shown) to negate the effects of the low regional structural plunge (avg 16°, S16W). In this view the batholith clearly possesses a concordant, sill-like structure at higher structural levels (northern half of EQD, fig. 3) and becomes discordant at lower structural levels (southern half of EQD, fig. 3) (Allison, ms). The above structural implications are that the EQD, along with its metasedimentary host, are facing upward,

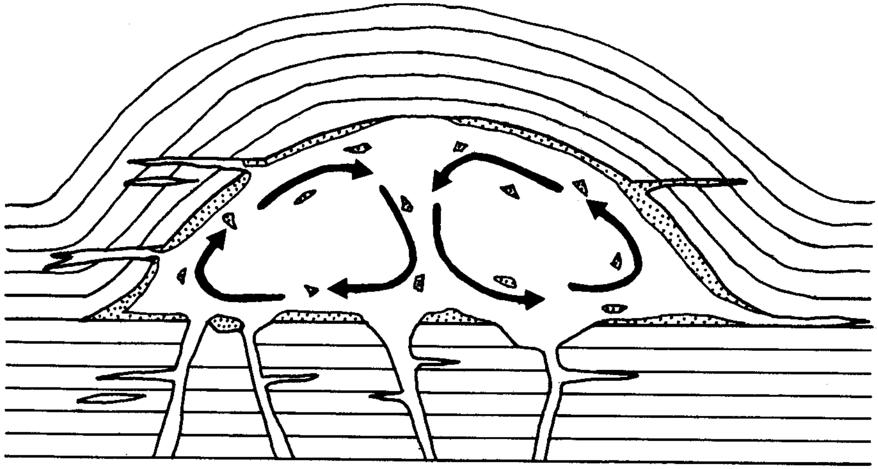

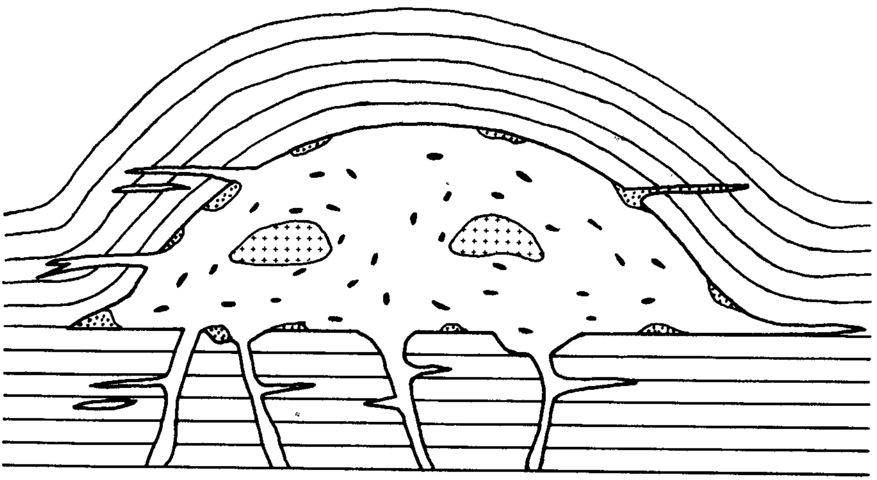

Fig. 6. Schematic diagram of the proposed laccolithic EQD magma chamber and crystallization effects. (A) Depiction of the convecting EQD magma chamber with attendant sidewall crystallization of gabbro-diorite cumulate enclave material (dotted pattern). Cumulate material is considered to have been mechanically mixed into the evolving and inward crystallizing EQD magma chamber. (B) Final crystallization leads to a batholithic body with normal zonation of dismembered gabbro-diorite enclaves scattered along the outer periphery, dominant tonalite-granodiorite comprising the main mass of the laccolith, and centalized bodies of highly felsic granitoids (+ pattern). Convective mixing of the gabbro-diorite enclave into the interior of the magma chamber involves reaction and inversion of these bodies to the common schistose enclaves (black ellipses) found scattered throughout the tonalite-granodiorite.

which is important in light of the lack of sedimentary structures in this high grade metamorphic terrane.

Tull (1987) has also pointed out the closely concordant nature of the EQD with surrounding Wedowee host rock stratigraphy, supporting its interpreted conformable laccolithic intrusive form. The western and northern contacts of the EQD are strongly interdigitated with the Wedowee Group metasedimentary rocks due both to a series of southwest to northeast doubly plunging, northwest verging F_3 folds (fig. 3) and to small intrusions of granitic material invading the schist from the main intrusive mass. The EQD's eastern contact is pervasively mylonitic due to faulting along the Alexander City fault (fig. 3). EQD gneisses and Emuckfaw-Heard schists are texturally degraded into blastomylonites and phyllonites, respectively, on the eastern margin. The Alexander City fault in the study area is a high angle fault (75°-90° dips) zone with both normal and right-lateral components of slip. Faulting along the Alexander City fault has tectonically removed an unknown portion of the EQD along its eastern terminus. The northern termination of the EQD is the result of a northeast-plunging F_3 fold closure. Concordance of the Wedowee stratigraphy with the EQD continues around the northern terminus where Wedowee stratigraphy can be traced around the fold hinge (Tull, 1987). Coastal plain clastics noncomformably overlie the EQD along its southern border. Thus, the 880 km^2 outcrop area of the EQD is a minimum estimate.

Structural interpretation.—The mapped region (fig. 3) has undergone multiple episodes of deformation and metamorphism. The earliest phase of deformation (D_1) accompanied prograde regional metamorphism (M_1) producing a pervasive S_1 foliation, L_{1M} mineral lineation, and F_1 flow folds. Mineral lineations are common in the EQD and consist mostly of quartz and feldspar but also of elliptical biotite grains and hornblende. The predominant phase of folding in the study area is F_3 which is coaxial with F_1 and L_{1M} (Tull, 1978; Drummond, ms). D_3 is represented by flexural-slip folds (F_3) ranging in size from crenulations to tight megascopic folds, all of which are doubly plunging northeast to southwest and overturned to the northwest. F_3 folds are most easily recognized near the margins of the batholith where significant infolding of metasedimentary rock delineates the fold surface geometry. A final cross folding event, F_4, consists of open (140°), megascopic flexural-slip folds that obliquely cut across earlier structural grain producing fold interference in the map pattern. Megascopic F_3 folding and F_4 cross folding creates the dominant structure in the study area, a series of interference basin and dome structures.

Emplacement of the EQD.—In a multiply deformed batholith, such as the EQD, emplacement mechanisms become difficult to interpret. However, the following lines of evidence point to a consistent model of emplacement for the EQD. (1) As discussed earlier, the presence of EQD veins crosscutting metadacite exposures implies that upper portions of the EQD may have intruded the base of its coeval hypabyssal-volcanic cover. An alternative view would be that the metadacite was pre-EQD and interlayered with the Wedowee host rocks. We oppose this alternative hypothesis because we have not observed the metadacites within the Wedowee Group and only find the metadacites totally encompassed within the EQD gneisses. The structural sites of the metadacites are in the upper concordant carapace of the laccolithic geometry, which is to be expected for an overlying hypabyssal-volcanic pile. Because of the minor amount of hypabyssal-volcanic material present (three small outcrop occurrences), the EQD may have barely pierced into the hypabyssal-volcanic pile before becoming gravitationally static. (2) Hornblende barometry indicates crystallization pressures from 4 kb possibly to as low as 1 kb indicating a mesozonal to epizonal intrusive environment. (3) The concordance of the structurally higher levels of the EQD with Wedowee stratigraphy, as shown by the northern termination (fig. 3), suggests that the batholith's final mode of emplacement did not allow it to crosscut stratigraphic layering. The concordant, tabular sill-like form of the EQD suggests permissive intrusion of an original laccolithic mass modified by superposed deformation. (4) Moore, Tull, and Allison (1987) suggested on the basis of a detailed strain analyses of the EQD, schistose enclaves, and crosscutting granitic dikes that pre-Acadian compressive deformation of the EQD was minimal. This observation is consistent with a permissive, extensional emplacement regime rather than a compressive tectonic environment for the EQD.

The above lines of evidence point to a subvolcanic, mesozonal to epizonal depth of emplacement for the EQD. The mode of emplacement is interpreted to be a permissive intrusion style associated with extensional tectonics. Final emplacement may have been accomplished by block stoping and roof uplift. At one locality (E331, S ½. SW ¼ sec 3, T.22N., R.21E., Alexander City quadrangle), the mechanical process of block stoping is well demonstrated where late-stage, cogenetic trondhjemitic magma has been injected between blocks of mafic tonalite. The tonalite has been wedged apart and segregated as angular blocks surrounded by a trondhjemite host. All the above physical features of the EQD are consistent with the three stages of ascent predicted by quantitative laccolith emplacement models (Corry, 1988), which are: (1) initial ascent as vertical dikes, (2) a transition from vertical to horizontal magma injection as sills, and (3) inflation and roof doming (Paterson, Vernon, and Fowler, 1991).

Many sites of batholith formation in an oceanic-continental convergent setting generally lack compressive tectonic features, for example, Boulder batholith, Montana (Hamilton and Myers, 1974) and Peruvian Coastal batholith (Pitcher, 1978; Bussell and Pitcher, 1985). Rather, they illustrate extensional tectonic features with passive intrusive mechanisms, such as roof uplift and block stoping. The Boulder batholith and Peruvian Coastal batholith are overlain by and intrude cogenetic volcanic cover several kilometers thick (generally 1-5 km). The features described above are consistent with those displayed by the EQD. A possible modern analogue to the intrusive style of the EQD may be the granitic magma bodies emplaced beneath the Long Valley caldera, California. Seismic studies have shown that the Long Valley magma bodies extend from 4.5 to at least 13 km depth ($\cong$1.5-5 kb pressure) (Sanders, 1984), and undoubtedly the upper portion of the Long Valley magma chamber is emplaced low into the overlying volcanic sequence.

IGNEOUS PETROGENESIS

Analytical methods.—Ninety-six whole-rock analyses on the EQD and associated lithologies have been utilized in this petrogenetic evaluation. Fourteen of these analyses and a description of the analytical methods were reported by Drummond (ms and 1987). The remaining 82 samples were recently analyzed by means of XRF (all major and minor elements, Cr, Rb, Sr, and Zr), ICP (Ba, Sc, Y, V, Nb, Co, Ni, Cu, Zn, Li, Be, and B), ICP-MS (U, Th, fourteen REEs), and INAA (Ta) by X-Ray Assay Laboratories, Toronto, Canada. Accuracy and precision estimates were made by blind and replicate analyses, respectively, of the Ailsa Craig granite IWG standard (AC-E) and United States Geological Survey diabase standard W-2, as shown in the appendix. Representative whole-rock major, minor, and trace element concentrations for the EQD and associated lithologies as listed in table 7.

Mafic enclaves—petrogenetic significance.—Scattered throughout the EQD are meter- to centimeter-size mafic enclaves. As will be shown later, the mafic enclaves play an important role in interpreting the igneous petrogenesis of the EQD. They not only record an early portion of the EQD's crystallization history but also demonstrate aspects of the dynamic magmatic conditions during crystallization. The general two-dimensional outline of the enclaves is subround to elongate ellipsoidal with the degree of ellipticity acting as a strain marker for the prekinematic EQD. These elongate enclaves are approximately coaxial with the dominant stretching lination (L_1)/mineral lineation (L_{1m}) pervasive throughout the EQD (Moore, Tull, and Allison, 1987).

There are two suites of mafic enclaves in the EQD: biotite–epidote–plagioclase schistose enclaves and hornblende–biotite gabbro–diorite enclaves. The lithologic, field, and textural information on the two enclave types was presented in the "Lithologic Description" section. A well-developed cumulate texture in the gabbro-diorite enclaves supports an igneous origin. On a macroscopic scale, the schistosity, biotite-rich character, and recrystallization in the schistose enclaves would suggest a metasedimentary xenolith interpretation. However, as discussed above, obvious metasedimentary septa enclosed by the EQD are mineralogically distinct from the schistose enclaves. We present four lines of geochemical evidence supporting an igneous origin for the schistose enclaves. (1) Shaw (1972) devised a geochemical (major element) test that discriminates between gneisses of probable igneous and metasedimentary origin. The schistose enclaves give positive "Shaw values," supportive of an igneous origin. (2) The EQD enclaves and host granodiorite and tonalite

TABLE 7

Representative chemical analyses of the EQD complex

A. Tonalites and Granodiorites

Sample	E328	CH2160	MD609	E181	E25	E502A	E239
SiO_2	62.5	63.0	63.5	63.9	64.4	64.8	65.0
TiO_2	0.63	0.72	0.61	0.54	0.65	0.61	0.62
Al_2O_3	18.1	17.8	16.7	17.4	17.2	17.3	17.1
Fe_2O_3	1.66	1.79	1.68	1.81	1.68	1.69	1.63
FeO	2.57	2.88	2.61	2.84	2.64	2.53	2.49
MnO	0.06	0.07	0.08	0.07	0.07	0.06	0.07
MgO	2.12	2.09	1.94	2.27	1.82	1.74	1.73
CaO	5.01	4.38	4.34	4.19	4.00	3.87	4.02
Na_2O	4.38	3.74	4.02	3.98	4.00	4.15	4.11
K_2O	1.95	2.16	2.01	2.13	2.01	2.26	2.15
P_2O_5	0.24	0.24	0.23	0.26	0.20	0.29	0.20
LOI	0.85	1.16	1.47	0.77	1.08	1.03	0.93
TOTAL	100.07	100.01	99.19	100.16	99.75	100.33	100.05
Trace elements (in ppm)							
Rb	80	110	100	100	100	160	90
Sr	990	660	730	730	680	570	720
Ba	600	740	480	680	880	225	710
Sc	7.5	10.9	9.4	8.6	9.9	8.0	9.2
Zr	180	190	180	140	170	165	180
Y	14	10	14	13	12	11	13
V	77	82	76	72	70	60	66
Nb	6.5	5.7	1.4	6.6	9.0	13.5	9.0
Ta		1	1	1		2	
Cr	20	30	40	60	40	35	30
Co	36	47	43	35	45	38	33
Ni	32	36	25	31	40	14	30
Cu	9.8	6.7	4.8	14.5	10.7	6.4	6.3
Zn	67	84	76	94	79	77	76
Li	37	58	57	46	54	63	38
Be	2.6	3.0	2.5	2.3	2.1	4.8	2.2
B	6	3	5	9	8	10	<2
U		2	1	<1		2	
Th		9	5	7		5.5	
La		40.7	27.2	30.4		26.5	
Ce		81.7	53.6	60.1		51.4	
Pr		9.3	5.7	6.6		5.7	
Nd		37.5	23.3	28.3		24.7	
Sm		6.0	4.3	5.3		4.8	
Eu		1.56	1.21	1.23		0.98	
Gd		4.2	3.3	4.1		3.5	
Tb		0.5	0.5	0.6		0.5	
Dy		2.6	2.7	3.2		2.4	
Ho		0.43	0.50	0.57		0.43	
Er		0.6	1.3	1.5		1.1	
Tm		0.1	0.2	0.2		0.1	
Yb		0.6	1.0	1.1		0.6	
Lu		0.08	0.14	0.14		0.09	

are metaluminous rather than peraluminous, which argues against a metasedimentary origin. (3) Rare earth elements behave relatively immobile during metasomatic processes (Muecke, Pride, and Sarkar, 1977), unlike major element criteria given above. Figure 7C compares chondrite-normalized REE patterns for both a diorite and schistose enclave, exhib-

TABLE 7
(continued)

A. Tonalites and Granodiorites

Sample	E573	E344	E343	E536	E628	E834	E391
SiO_2	65.3	65.6	65.9	66.2	66.4	66.4	66.6
TiO_2	0.62	0.62	0.59	0.57	0.55	0.56	0.53
Al_2O_3	17.2	16.9	17.2	16.7	16.8	16.9	16.8
Fe_2O_3	1.63	1.61	1.56	1.54	1.51	1.41	1.42
FeO	2.49	2.50	2.35	2.22	2.25	2.19	2.10
MnO	0.07	0.06	0.06	0.06	0.07	0.06	0.07
MgO	1.76	1.67	1.60	1.49	1.59	1.82	1.53
CaO	3.97	3.90	3.84	3.43	3.57	3.98	3.49
Na_2O	4.29	4.11	4.25	4.06	4.20	4.31	4.13
K_2O	1.97	1.98	2.09	2.61	2.18	1.74	2.39
P_2O_5	0.20	0.20	0.19	0.19	0.21	0.20	0.19
LOI	0.62	0.77	0.62	0.70	0.77	0.70	0.70
TOTAL	100.12	99.92	100.25	99.77	100.10	100.27	99.95

Trace elements (in ppm)

Rb	120	90	100	120	130	140	110
Sr	650	680	690	600	560	630	580
Ba	400	580	590	770	340	260	470
Sc	9.2	8.7	8.8	8.4	8.1	7.8	8.1
Zr	180	180	180	180	160	160	150
Y	13	11	8.5	8.0	7.8	7.3	8.7
V	66	58	57	53	55	57	53
Nb	8.2	8.4	5.1	8.8	8.6	7.6	5.4
Ta				1	1		
Cr	40	30	30	30	40	50	30
Co	39	32	38	35	42	42	43
Ni	20	26	27	34	15	17	21
Cu	8.1	7.7	3.6	7.7	6.2	11.0	10.3
Zn	72	69	70	72	74	66	65
Li	32	50	41	34	60	64	52
Be	3.2	1.9	2.2	3.2	4.0	3.4	2.9
B	7	7	4	9	4	<2	6
U				2	2		
Th				9	7		
La				33.2	28.2		
Ce				66.3	53.3		
Pr				7.5	6.3		
Nd				29.6	24.5		
Sm				5.4	4.5		
Eu				1.25	1.14		
Gd				3.7	3.3		
Tb				0.5	0.4		
Dy				2.2	2.0		
Ho				0.33	0.29		
Er				0.8	0.7		
Tm				<0.1	<0.1		
Yb				0.4	0.5		
Lu				0.05	0.06		

iting virtually identical REE patterns between the two enclave types. (4) On Harker diagrams (fig. 8A-D) the schistose enclaves consistently fall between tonalite and gabbro-diorite enclave compositions. This relationship suggests that the schistose enclaves may have been original gabbro-diorite enclaves metasomatized by coexisting EQD magma. Figure 8D

TABLE 7

(continued)

A. Tonalites and Granodiorites

Sample	E654	E36	E769	E448	E591	E797	E618
SiO_2	66.8	66.8	67.1	67.2	67.4	67.6	68.0
TiO_2	0.54	0.50	0.47	0.47	0.50	0.45	0.42
Al_2O_3	16.3	16.7	15.7	16.5	16.7	16.7	17.0
Fe_2O_3	1.45	1.39	1.30	1.24	1.24	1.29	1.16
FeO	2.19	2.00	1.91	1.93	1.92	1.86	1.66
MnO	0.07	0.07	0.05	0.06	0.05	0.06	0.06
MgO	1.49	1.41	1.54	1.40	1.36	1.31	1.04
CaO	3.54	3.53	3.12	4.20	3.23	3.13	3.33
Na_2O	4.06	4.08	4.57	4.27	4.10	4.23	5.05
K_2O	2.12	2.57	1.81	1.68	1.83	2.42	1.60
P_2O_5	0.18	0.18	0.15	0.16	0.13	0.25	0.07
LOI	1.23	0.77	1.70	0.70	1.47	1.08	0.70
TOTAL	99.97	100.00	99.42	99.81	99.93	100.38	100.09

Trace elements (in ppm)

Rb	120	120	100	80	80	150	130
Sr	600	650	520	780	680	500	480
Ba	470	1000	260	610	640	350	130
Sc	8.4	7.9	6.3	4.8	7.3	6.7	5.3
Zr	170	160	220	130	150	130	110
Y	10	16	11	6.3	8.1	9.4	2.1
V	58	55	42	53	49	42	40
Nb	8.8	6.2	8.3	5.5	7.2	9.8	8.0
Ta							
Cr	40	30	30	20	30	30	30
Co	44	42	41	43	46	42	43
Ni	23	44	16	22	24	17	10
Cu	6.5	4.5	10.7	2.3	4.6	4.0	3.4
Zn	67	69	73	59	55	65	65
Li	71	71	42	32	40	46	50
Be	4.0	3.6	2.5	2.7	2.2	3.5	5.1
B	10	6	<2	6	6	4	2
U							
Th							
La							
Ce							
Pr							
Nd							
Sm							
Eu							
Gd							
Tb							
Dy							
Ho							
Er							
Tm							
Yb							
Lu							

shows that representative Wedowee Group metasedimentary rock compositions (Drummond, ms) typically fall at extremely low (< 1 wt percent) CaO contents over a range of SiO_2 values. Thus, schistose enclave compositions cannot be explained by linear mixing between host EQD tonalitic magma and partially assimilated Wedowee Group country rock.

TABLE 7
(continued)

A. Tonalites and Granodiorites

Sample	E480	E607	E89	E138	E85	E410	E11
SiO_2	68.5	68.7	69.3	69.5	70.1	70.9	71.6
TiO_2	0.42	0.47	0.44	0.36	0.32	0.33	0.34
Al_2O_3	16.1	16.1	16.1	16.0	15.8	15.0	15.0
Fe_2O_3	1.17	1.25	1.07	1.10	0.83	1.00	0.89
FeO	1.81	1.91	1.74	1.43	1.11	1.45	1.34
MnO	0.05	0.06	0.05	0.06	0.05	0.05	0.04
MgO	1.22	1.31	1.33	0.90	0.84	0.97	0.85
CaO	3.51	3.41	3.98	2.41	2.66	2.86	2.52
Na_2O	4.11	4.47	4.20	4.01	4.25	4.00	3.50
K_2O	1.79	1.66	1.38	3.45	2.89	2.31	3.03
P_2O_5	0.20	0.11	0.11	0.09	0.08	0.09	0.07
LOI	1.16	0.70	0.54	0.77	1.00	0.54	0.77
TOTAL	100.04	100.15	100.24	100.08	99.93	99.50	99.95

Trace elements (in ppm)

Rb	100	80	70	130	100	100	90
Sr	580	590	740	480	660	540	480
Ba	480	290	460	810	1200	560	970
Sc	5.8	7.1	6.7	6.3	5.6	5.6	6.1
Zr	150	150	130	120	100	110	90
Y	8.1	7.2	6.5	26	7.0	9.3	17
V	42	48	51	27	34	32	33
Nb	6.4	7.2	5.4	9.1	6.4	7.7	9.0
Ta							1
Cr	20	30	30	10	30	30	30
Co	45	43	38	40	44	42	45
Ni	16	12	23	29	44	20	36
Cu	2.1	5.5	4.4	1.3	2.3	1.5	3.4
Zn	57	59	53	59	38	46	43
Li	36	49	39	41	47	43	36
Be	3.0	3.7	2.4	3.0	2.4	2.6	2.4
B	<2	14	10	9	8	13	7
U							2
Th							11
La							25.4
Ce							53.0
Pr							6.4
Nd							25.2
Sm							5.1
Eu							1.18
Gd							4.4
Tb							0.6
Dy							3.5
Ho							0.64
Er							1.8
Tm							0.2
Yb							1.4
Lu							0.22

Thus, on the basis of this mineralogical and chemical evidence, an igneous origin is also interpreted for the schistose enclaves.

If these enclaves are of igneous heritage, then what is their petrogenetic significance to the magmatic evolution of the EQD? Before this question can be addressed we will first document the four common modes of mafic enclave origin and their characteristic features.

TABLE 7

(continued)

B. Leucocratic Elkahatchee gneisses

Sample	E141	E322B	E462	E579	E667
SiO_2	74.0	74.0	68.4	68.6	72.8
TiO_2	0.08	0.09	0.37	0.43	0.20
Al_2O_3	15.1	15.0	16.2	16.2	15.0
Fe_2O_3	0.30	0.23	1.05	1.29	0.68
FeO	0.36	0.29	1.25	1.94	0.84
MnO	0.03	0.03	0.05	0.05	0.05
MgO	0.20	0.20	1.01	0.87	0.47
CaO	1.71	1.91	2.31	2.33	1.34
Na_2O	6.01	5.95	3.28	4.01	4.18
K_2O	1.83	1.68	4.94	2.01	3.53
P_2O_5	0.06	0.08	0.17	0.15	0.23
LOI	0.31	0.47	0.62	2.23	0.93
TOTAL	99.99	99.93	99.65	100.11	100.25

Trace elements (in ppm)

Rb	60	50	130	100	190
Sr	710	800	660	330	300
Ba	360	320	2400	440	530
Sc	2.6	1.7	5.7	4.1	3.1
Zr	30	50	100	180	80
Y	5.1	3.0	10	6.2	8.4
V	4	3	43	27	12
Nb	3.2	1.1	6.5	10	9.3
Ta	1				
Cr	20	20	20	20	20
Co	48	44	48	40	29
Ni	11	15	79	15	21
Cu	2.9	1.5	2.9	<0.5	1.7
Zn	23	22	47	100	75
Li	46	23	58	29	68
Be	3.0	1.2	2.5	2.5	6.0
B	4	5	<2	9	15
U	2				
Th	6				
La	17.7				
Ce	34.4				
Pr	3.6				
Nd	15.4				
Sm	2.7				
Eu	0.52				
Gd	1.6				
Tb	0.2				
Dy	1.1				
Ho	0.20				
Er	0.5				
Tm	<0.1				
Yb	0.4				
Lu	0.07				

1. Mixing and/or mingling between introduced mafic magma and host granitic magma. The mixing hypothesis for mafic enclave development in granitic rocks is presently a well accepted model (Didier and Barbarin, 1991). Texturally, this type of mafic enclave will typically exhibit some or all the following characteristics: chilled contacts, crenu-

TABLE 7

(continued)

	C. Non-cogenetic felsic granitoids				D. Metadacites		
Sample	E135	E142	E502C	E841	E223	E262	E604
SiO_2	70.3	72.4	69.9	68.5	72.5	70.4	70.9
TiO_2	0.20	0.05	0.20	0.29	0.21	0.20	0.21
Al_2O_3	16.3	15.9	16.3	16.1	15.7	16.6	16.2
Fe_2O_3	0.56	0.22	0.49	0.82	0.51	0.45	0.51
FeO	0.73	0.23	0.56	0.95	0.66	0.59	0.64
MnO	0.03	0.02	0.03	0.04	0.03	0.02	0.02
MgO	0.54	0.13	0.51	0.86	0.51	0.51	0.46
CaO	2.82	1.11	2.11	2.32	1.95	2.11	1.76
Na_2O	4.25	5.10	5.46	3.49	5.01	5.44	5.22
K_2O	3.15	4.04	2.98	5.03	2.19	1.77	2.30
P_2O_5	0.16	0.06	0.09	0.27	0.10	0.10	0.09
LOI	1.00	0.54	1.77	1.16	0.70	2.00	1.47
TOTAL	100.04	99.80	100.40	99.83	100.07	100.19	99.78

Trace elements (in ppm)

Rb	90	70	90	150	50	50	50
Sr	680	620	920	620	870	830	830
Ba	1000	2700	600	1600	590	430	510
Sc	3.5	3.6	2.2	4.2	2.7	2.6	2.4
Zr	110	20	90	80	80	80	90
Y	11	4.4	3.8	9.7	3.5	3.3	4.3
V	17	<1	16	30	16	18	11
Nb	5.3	2.5	3.2	5.4	2.5	2.2	2.2
Ta				1	<1		
Cr	10	20	30	20	30	20	20
Co	38	53	40	56	28	27	22
Ni	31	83	19	54	23	20	16
Cu	0.7	0.7	0.5	3.5	2.4	1.9	0.7
Zn	31	17	42	44	40	36	42
Li	41	35	45	45	22	33	37
Be	2.4	1.3	2.1	3.0	1.6	1.5	1.6
B	<2	3	10	5	10	6	3
U				<1	<1		
Th				7	3		
La				32.3	5.6		
Ce				63.2	8.5		
Pr				7.0	1.2		
Nd				28.1	5.2		
Sm				4.9	1.1		
Eu				1.15	0.33		
Gd				3.6	0.8		
Tb				0.5	0.1		
Dy				2.1	0.8		
Ho				0.36	0.13		
Er				0.9	0.4		
Tm				<0.1	<0.1		
Yb				0.5	0.4		
Lu				0.06	0.05		

E135 - Bluff Springs Granite, E502C - fine-grained trondhjemitic dike, E142 - muscovite leucogranite, and E841 - biotite quartz monzonite

late margins, acicular apatite, rapikivi texture, rounded quartz xenocrysts ("ocelli") with biotite-hornblende coronas, and plagioclase with resorbed cores and dendritic overgrowths (Vernon, 1990; Castro, Moreno-Ventas, and de la Rosa, 1990). None of the above textural features is

TABLE 7
(continued)

E. Gabbro-Diorite Enclaves					F. Schistose Enclaves		
Sample	E33	E40	E204	E792	E331A	E715B	E740B
SiO_2	51.7	56.3	55.7	54.7	60.0	57.3	55.8
TiO_2	0.69	0.74	0.82	1.31	0.75	1.36	0.79
Al_2O_3	15.4	16.8	17.0	16.9	17.6	17.4	18.2
Fe_2O_3	2.29	2.31	2.44	2.33	2.19	2.70	2.93
FeO	5.14	4.05	3.40	4.69	3.35	4.72	4.74
MnO	0.13	0.12	0.15	0.11	0.09	0.14	0.16
MgO	8.20	5.09	3.76	5.42	2.98	2.61	3.73
CaO	10.30	6.38	6.78	8.44	4.90	6.62	5.83
Na_2O	2.86	3.33	3.24	3.56	3.92	3.31	2.89
K_2O	0.90	2.12	4.27	0.96	2.60	2.21	3.36
P_2O_5	0.13	0.22	0.32	0.20	0.19	0.26	0.28
LOI	2.23	1.39	1.16	1.54	1.23	1.77	1.70
TOTAL	99.97	98.85	99.04	100.16	99.80	100.40	100.41

Trace elements (in ppm)

	E33	E40	E204	E792	E331A	E715B	E740B
Rb	30	80	110	40	100	100	200
Sr	880	860	810	880	580	760	530
Ba	110	580	1200	180	510	420	530
Sc	27.0	17.9	18.7	15.4	11.7	15.3	22.6
Zr	30	140	180	70	130	170	150
Y	15	21	38	13	16	27	30
V	120	120	120	92	96	140	150
Nb	4.8	8.0	8.4	2.5	7.3	13	6.5
Ta		<1	1			1	
Cr	290	210	20	90	10	10	20
Co	53	45	34	41	34	37	39
Ni	42	66	48	57	23	14	25
Cu	44.3	22.7	24.0	9.9	4.0	11.5	16.2
Zn	72	79	95	66	77	87	120
Li	34	53	39	27	37	73	100
Be	2.5	2.1	2.8	2.1	2.1	2.8	3.0
B	4	<2	7	5	5	3	8
U		<1	2			2	
Th		5	3			7	
La		27.0	28.7			30.8	
Ce		59.5	66.6			65.6	
Pr		6.9	8.7			8.0	
Nd		31.8	44.0			34.5	
Sm		6.5	10.6			7.1	
Eu		1.65	2.13			1.89	
Gd		5.6	9.9			6.1	
Tb		0.8	1.5			0.9	
Dy		4.7	8.6			5.6	
Ho		0.91	1.63			1.05	
Er		2.6	4.4			3.1	
Tm		0.4	0.6			0.5	
Yb		2.3	3.6			2.8	
Lu		0.32	0.49			0.39	

present in the EQD's enclaves arguing against their origin via magma mingling.

2. Introduction of enclaves as xenolithic country rock. The general lack of mafic igneous rocks or their metamorphic equivalents in the exposed country rock to the EQD argues against a xenolithic origin for the mafic enclaves.

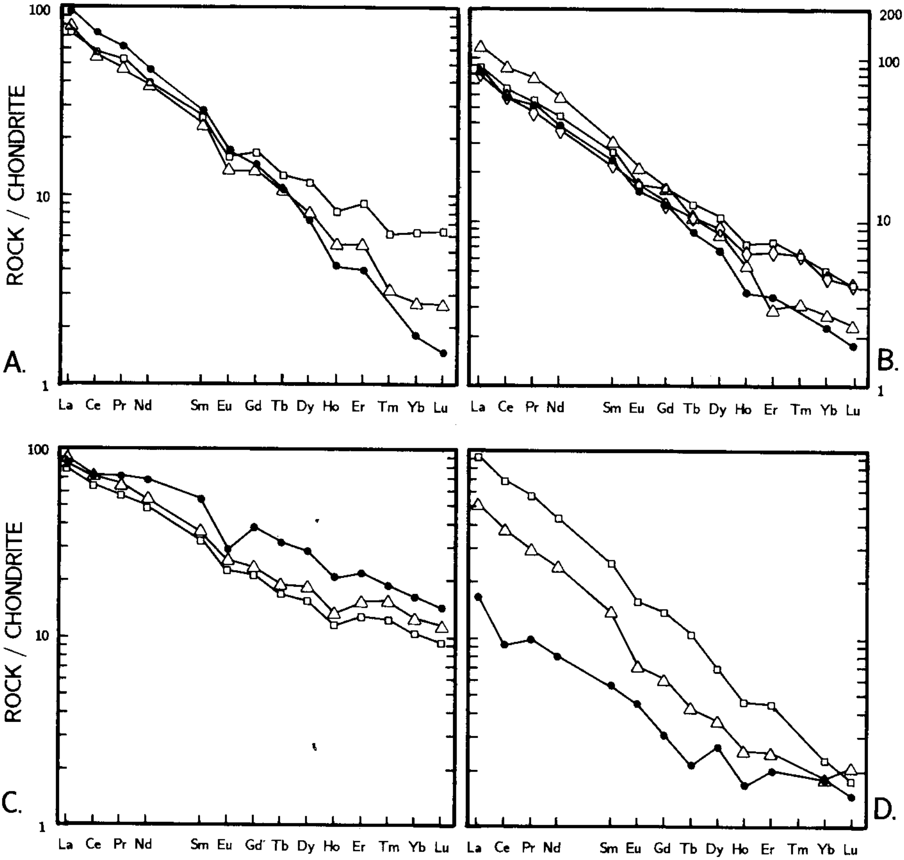

Fig. 7. Chondrite-normalized (Wakita, Rey, and Schmitt, 1971) REE patterns of the EQD complex. (A) Granodiorites: square = E11, triangle = E502A, closed circle = E536; (B) tonalites: square = E180, triangle = CH2160, diamond = MD609, closed circle = E628; (C) enclaves: square = E40 (diorite), triangle = E715B (schistose), closed circle = E204 (monzodiorite); (D) felsic granitoids and metadacite: square = E841, triangle = E141, closed circle = E223, metadacite. Complete geochemical analyses of each sample is listed in table 7.

3. Restite origin. Chen and others (1990) report characteristics of mafic enclaves of presumed restite origin from I-type granites of the Lachlan Fold Belt, Australia. Significant distinctions between the features described for restite enclaves and enclaves of the EQD are as follows: (A) the restite enclaves are limited in size to about 1 m, whereas EQD gabbro-diorite enclaves range up to tens of meters in diameter; and (B) the restite enclaves are not restricted to the pluton's margin but are scattered throughout, whereas the EQD enclaves are concentrated near the batholith's margins.

4. Cumulate process. The most viable interpretation for the EQD's mafic enclaves is by a cumulate enrichment process. This hypothesis can explain the gabbro-diorite enclaves exhibiting a cumulate texture and grain size similar to or coarser than the host granitoid. Although the enclaves contain higher proportions of mafic minerals, mineralogically they are similar to the host EQD. Other studies that favor a cumulate origin for mafic enclaves in I-type granitoid bodies include Pitcher (1978), Coastal batholith, Peruvian Andes; Flood and Shaw (1979), Uralla pluton, New England batholith, Australia; and Dodge and Kistler (1990), Sierra Nevada batholith.

The two enclave types in the EQD, gabbro-diorite, and schistose enclaves, are found in separate geographic areas of the EQD batholith. The gabbro-diorite enclaves are found solely along the outer contact zones of the EQD. Schistose enclaves are scattered throughout the interior portions of the EQD but decrease in concentration toward the centralized leucocratic EQD zones (figs. 3 and 6).

A combination of cumulate texture, near-liquidus phase assemblage (hornblende + biotite + andesine primocryst) and location along the batholith's outer margin argues for early crystal accumulation via sidewall crystallization for formation of the gabbro-diorite enclaves. The discontinuous character of this cumulate material and sidewall crystallization processes implies that flowage differentiation occurred in a dynamic, convecting magma chamber. The high viscosity of granitic magmas severely limits the viability of cumulate processes in granitic magmas (Burnham, 1979), but dynamic, sidewall accumulation circumvents this physical constraint.

We consider the schistose enclaves to represent original gabbro-diorite enclaves convectively mixed into the EQD interior, mechanically disaggregated into smaller bodies, and reacted with more Si-, K-, and H_2O-rich later stage magmas. The transportation of the gabbro-diorite enclaves into the evolving, inwardly crystallizing granitic magma chamber created the conditions necessary for reaction 1 (see above) to produce the abundant epidote and biotite in the schistose enclaves. Coarse plagioclase primocrysts in the schistose enclaves are commonly poikilitic with abundant epidote and stubby apatite inclusions. Limited incorporation of phosphorus takes place in plagioclase by the coupled exchange $Al^{+3} + P^{+5} = 2Si^{+4}$ (London and others, 1990). Recrystallization of plagioclase in the schistose enclaves could allow $(PO_4)^{-4}$ exsolution and formation of apatite inclusions and poikilitic texture. These plagioclase primocrysts in the schistose enclaves may represent early crystallizing plagioclase that was transported into an environment of instability and recrystallization.

In conclusion, the enclaves are interpreted to represent disrupted fragments of cumulate material which formed as near-liquidus sidewall crystallization products. Active convection in the EQD magma chamber segmented the gabbro-diorite cumulates into discrete meter-size enclaves along the batholith's outer margin. Convective transportation of cumulate material into the interior of the evolving granitic magma chamber led

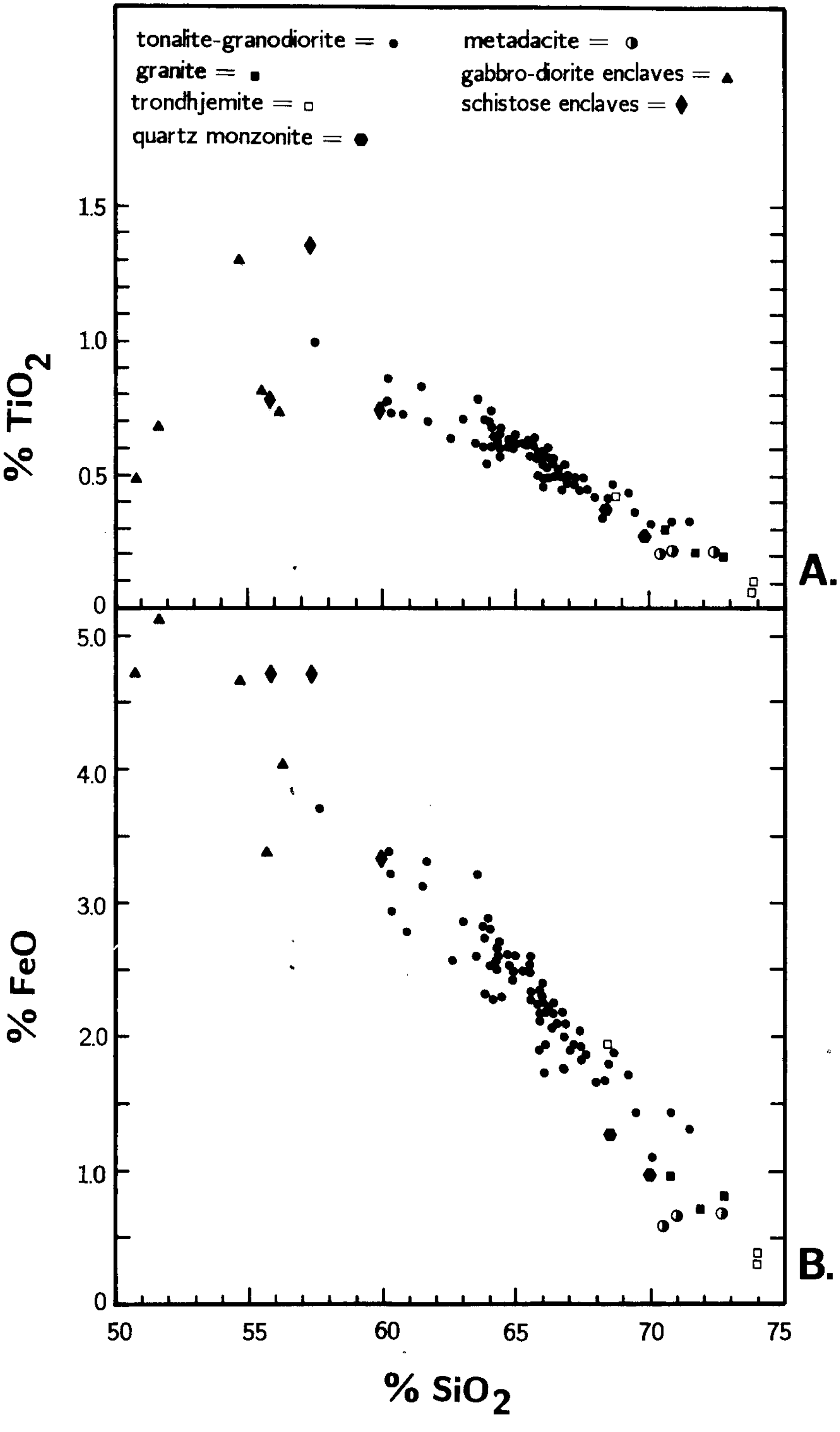

Fig. 8. Major and minor element Harker diagrams of those samples of the EQD complex considered to be cogenetic. On (8D), W stands for Wedowee Group metasediment compositions from Drummond (1986).

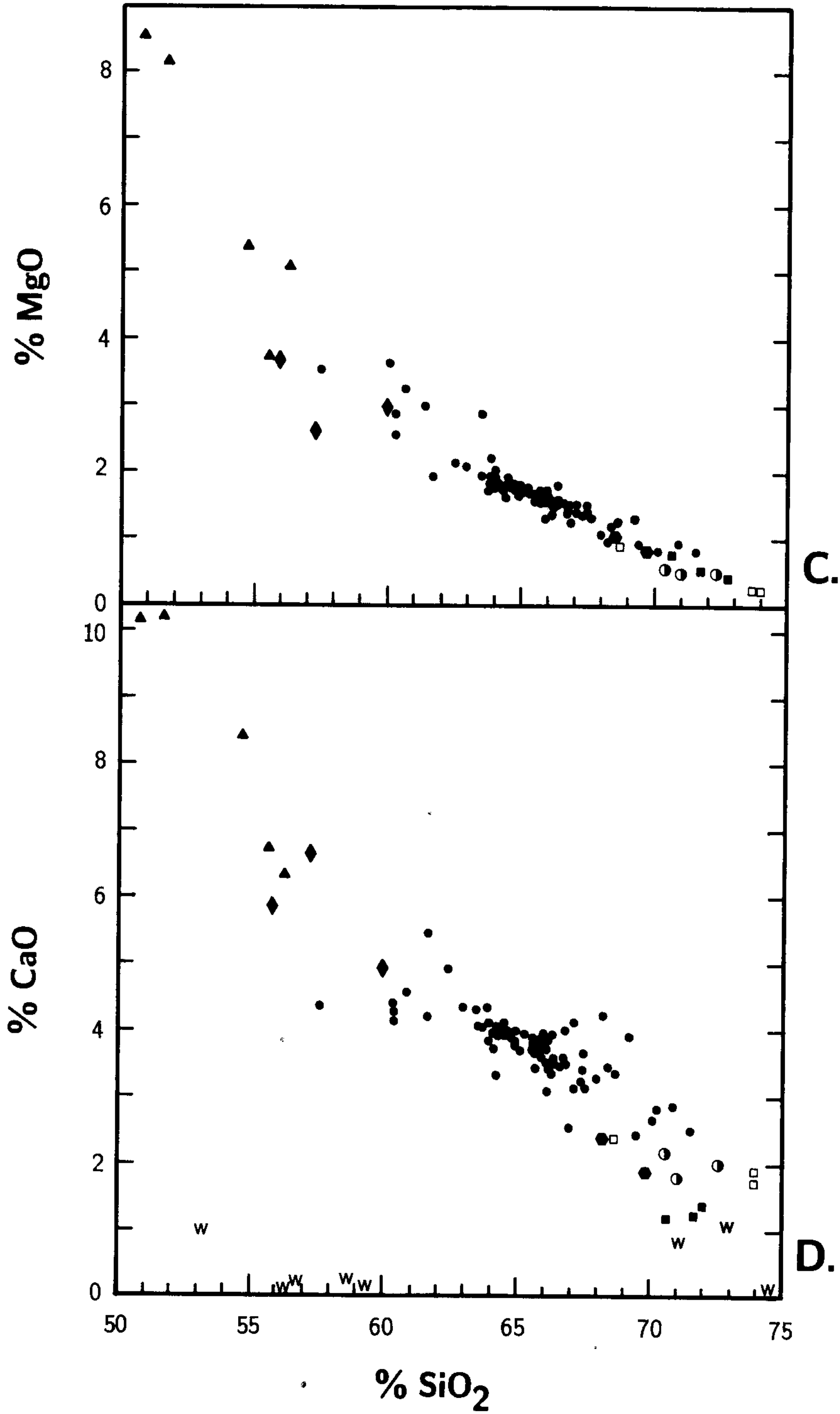

Fig. 8. (continued)

to mechanical disaggregation, solid-melt reaction, and ultimately biotite-epidote enclaves (fig. 6). Because of the biotite-rich nature of the biotite-epidote enclaves, superposed D_1-M_1 deformation produced a foliated fabric and flattened ellipsoidal shape.

Major element modeling.—Representative major and minor element Harker diagrams are shown in figure 8A to D. A broad range of SiO_2 (47-74 percent) is represented by the enclaves and granitoids of the EQD with the enclaves containing less than and the granitoids more than 60 percent SiO_2. The granodiorites, tonalites, and leucocratic Elkahatchee gneisses exhibit roughly linear variation trends, whereas the enclave samples comprise a scattered population at low SiO_2 values. Convective transport and chemical reequilibration of the cumulate material with a continuously evolving granitic melt phase could produce the compositional scatter of the enclaves. In addition, the amount of trapped intercumulus melt and variations in cumulate plagioclase versus cumulate mafic phase (clinopyroxene, hornblende, and biotite) abundance may provide some scatter within the enclave samples. Other studies that have called upon crystal fractionation and cumulate processes in intermediate to felsic magma petrogenesis have shown a compositional scatter among the cumulate material (Wyborn, Turner, and Chappell, 1987; Woodhead, 1988; Dodge and Kistler, 1990).

Major and minor element covariation can best be modeled by crystal fractionation, using a computer program (Geist, Baker, and McBirney, 1985) based upon the Wright and Doherty (1970) model for solving least squares mixing problems. A two-stage crystallization process was invoked to represent the changing proportions of crystalline phases with magma evolution. All mineral chemistries used in the calculations were from this study except for apatite, which was taken from Deer, Howie, and Zussman (1982). Whole-rock analyses of assumed parent and daughter products are given in table 7.

The first stage of crystal differentiation explains the compositional variation in the 60 to 67 percent SiO_2 range. Samples E328 and E628 (table 7) represent tonalites from either end of this low SiO_2 range. Mineral compositions and proportions were chosen to correspond with those phases found to crystallize early relative to the EQD's mineral paragenesis (table 6). The linear mixing calculations indicate that it is possible to produce E628 biotite tonalite from E328 biotite tonalite by 23 percent crystallization of a cumulate composed of 61 percent andesine primocrysts, 13 percent hornblende, 13 percent biotite [Fe/(Fe + Mg) = 35], 12 percent Fe-epidote, 1 percent apatite. The above proportions of crystallizing phases are similar to the mineral content in the gabbro-diorite enclaves, supporting a near-liquidus, cumulate origin for these enclaves. Compositional variation between 67 and 74 percent SiO_2 is modeled utilizing sample E628 as parent and E322B trondhjemite (74 percent SiO_2) as daughter. Mineral compositions and proportions were chosen for the model to represent those phases associated with the intermediate to late stage of the EQD's mineral paragenesis (table 6).

Seventy-seven percent crystallization of the extract assemblage, 50 percent andesine primocrysts, 26 percent quartz, 18 percent biotite [Fe/(Fe + Mg) = 56], 4 percent K-feldspar, 1 percent hornblende satisfy this second stage of EQD magma evolution. The above extract assemblage corresponds to the modal content in a typical EQD biotite tonalite-granodiorite. The first and second stage crystallization models give R^2 values (sum of squares of the residuals) of 0.042 and 0.037, respectively. R^2 values less than 0.1 are considered excellent solutions to the compositional model (Geist, Baker, and McBirney, 1985). Therefore, a parental EQD magma of E328 composition may produce the most felsic EQD endmember (E322B) by a two-step crystallization process requiring 82 percent total crystallization.

Additional major element relationships supporting the above least squares mixing model include the strong positive correlation (99.9 percent significance level) between all possible combinations of TiO_2, Fe_2O_3, FeO, MnO, MgO, CaO, Al_2O_3, and P_2O_5 and a strong negative correlation (99.9 percent significance level) between the above elements and SiO_2. These inter-element correlations are consistent with early hornblende, biotite, Fe-epidote, andesine primocryst, and apatite differentiation via crystal fractionation.

Trace element modeling.—Multiple regression of trace elements, along with major and minor elements, provides correlations that substantiate the least squares mixing calculations. For example, Sc, Zr, V, Y, Nb, Cr, Cu, and Zn exhibit strong negative correlations (99.9 percent significance level) with SiO_2 suggesting the early depletion of these elements by crystallization of hornblende, biotite, andesine primocrysts, Fe-epidote, and zircon.

The behavior of Rb and Sr relative to K and Ca, respectively, typically provides a useful petrogenetic profile of granitic magmas (Marshall and DePaolo, 1989). Granitoids with low Ca/Sr ratios suggest restite control or fractionation of phases that concentrate Ca (high Kd_{Ca}) relative to Sr (low Kd_{Sr}), such as hornblende (Kd_{Ca} = 1.8 and Kd_{Sr} = 0.23) and/or plagioclase (Kd_{Ca} = 3.4 and Kd_{Sr} = 1.8) (Gill, 1981; Henderson, 1982). Conversely, if Ca/Sr is high, then the magma differentiated phases with more strongly concentrated Sr relative to Ca, such as K-feldspar (Kd_{Ca} = 1.9 and Kd_{Sr} = 3.87; Philpotts and Schnetzler, 1970). K/Rb ratios in granitic magmas may be controlled by the fractionation of biotite (high K/Rb in melt; Kd_{Rb} = 3.26) and/or K-feldspar (low K/Rb in melt; Kd_{Rb} = 0.659) (Hanson, 1978).

The EQD demonstrates increasing K/Rb with fractionation (strong positive correlation between K/Rb and SiO_2, significance level = 99.9 percent) suggestive of biotite fractionation; whereas Ca/Sr decreases with increasing SiO_2 (strong negative correlation at significance level = 99.9 percent) as the result of hornblende and/or plagioclase fractionation. Figure 9 illustrates the EQD differentiation trend of decreasing Ca/Sr and increasing K/Rb with fractionation. The minor scatter of data in

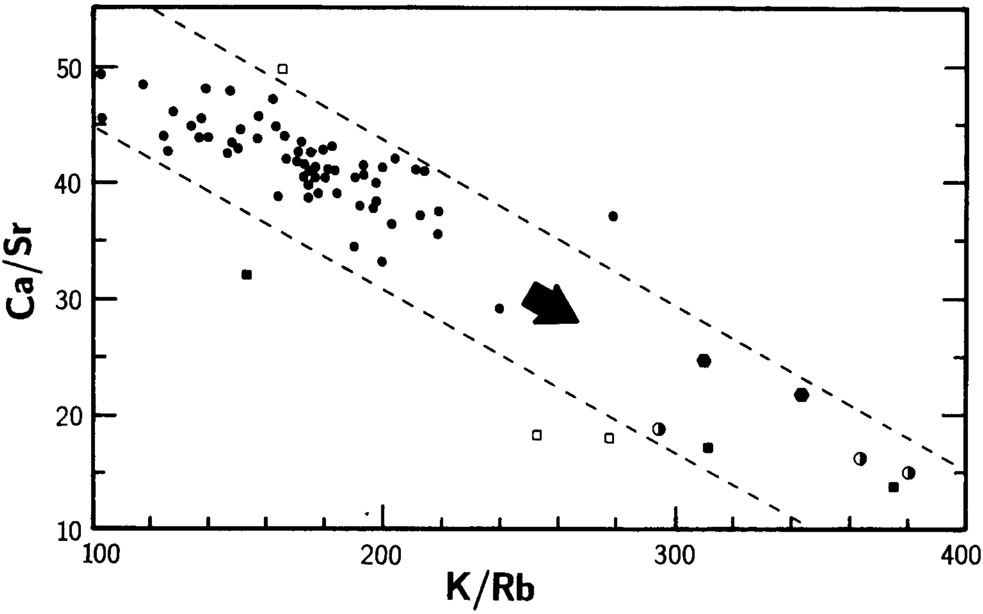

Fig. 9. K/Rb versus Ca/Sr of the EQD. Symbology same as that in figure 8. Arrow points in direction of magmatic differentiation; refer to text for discussion.

figure 9 is primarily restricted to felsic granitoids, presumably due to mobility of Rb and Sr by late stage granitic fluids.

The calc-alkaline, I-type tonalites-granodiorites, leucocratic gneisses, and metadacites of the EQD complex display trace element abundances characteristic of volcanic arc granitoids (Pearce, Harris, and Tindle, 1984; Harris, Pearce, and Tindle, 1986). For example, the tonalites-granodiorites, leucocratic gneisses, and metadacites all fall within the volcanic arc granitoid field with respect to the Y + Nb versus Rb (fig. 10), Y versus Nb, SiO_2 versus Rb (Pearce, Harris, and Tindle, 1984), and SiO_2 versus Rb/Zr (Harris, Pearce, and Tindle, 1986) tectonic discriminant trace element diagrams. Some of the leucocratic gneisses (table 7) and all the metadacites fall on the highly differentiated end on all Harker diagrams (fig. 8) and trace element diagrams (fig. 9), indicating a chemical continuity and interpreted cogenetic relationship with the tonalites-granodiorites of the EQD.

Source composition.—Geochemical and mineralogical characterization of a granitic source can be approximated utilizing REE geochemistry. The presence of applicable Kd's, relative immobility via secondary processes, and compatible behavior in a wide range of major and accessory phases allow REE modeling to be very useful in deducing granitic source material, refractory assemblage, and percent partial melt. Six mafic

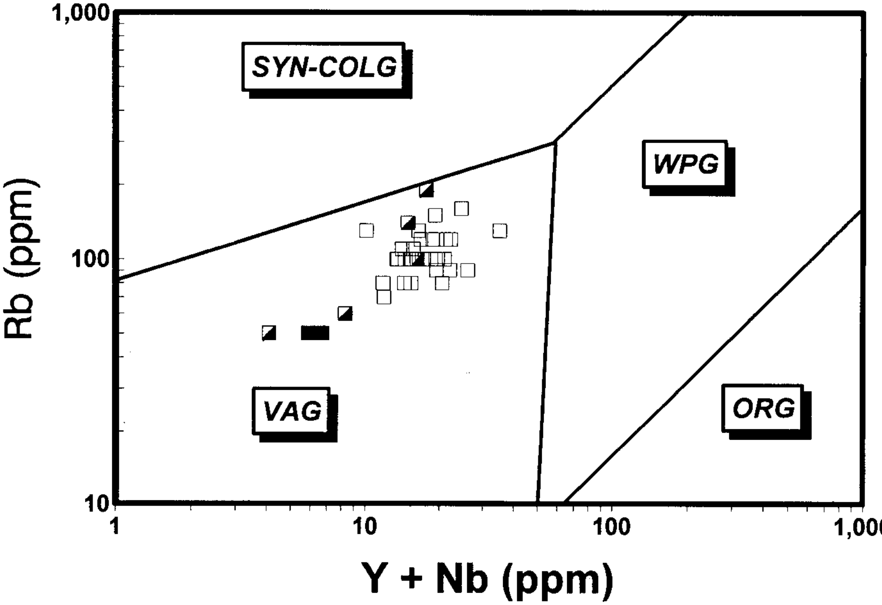

Fig. 10. Y + Nb versus Rb tectonic discriminant diagram (Pearce, Harris, and Tindle, 1984) of the EQD. Field explanation: SYN-COLG = syn-collisional granites, VAG = volcanic arc granites, WPG = within plate granites, and ORG = ocean ridge granites. Open squares = tonalite and granodiorite, filled squares = metadacite, and half-filled squares = trondhjemite and granite.

granodiorites and tonalites (63-66 percent SiO_2) with REE analyses (table 7) are assumed to represent reasonable estimates of the EQD's parental magma composition. These samples were chosen as representatives of the parental magma composition because they are neither cumulate crystal-bearing or highly differentiated. Chondrite-normalized REE patterns for granodiorites (fig. 7A), tonalites (fig. 7B), and enclaves (fig. 7C) exhibit a continuity of REE pattern within each group. Exceptions to this within-group similarity include a felsic granodiorite sample (E11, fig. 7A and table 7) and the felsic granitoids (fig. 7D). In these more felsic granitoids, REE behavior is more prone to control by accessory phases, such as zircon, apatite, and sphene, due to saturation of the magma in these critical phases with differentiation. The felsic granitoids will not be considered further in the estimation of EQD source material.

A number of different source materials were evaluated during the petrogenetic analysis. Given the I-type character of the EQD and the 63 to 66 percent SiO_2 level for the presumed parental magmas, intermediate to mafic source materials are reasonable candidates. Partial melting models of andesitic and basaltic source materials leaving amphibolitic or granulitic restite assemblages were not successful (Drummond, ms).

Recent experimental studies (Rapp, Watson, and Miller, 1991) have shown that tonalitic parental magmas can be produced with REE patterns similar to those in figure 7A by partial melting basalt at high pressure ($\geq$ 16 kb), leaving garnet–clinopyroxene–hornblende rich residues. We have tested this type of partial melting model below.

A geochemical model is presented in figure 11, in which a source consisting of 99.3 percent MORB (avg of 165 REE analyses from the literature, data compilation available upon request to the senior author) plus 0.7 percent deep-sea sediment (Shimokawa, Masuda, and Izawa, 1972; Hole and others, 1984) undergoes 10 to 30 percent partial melting. This model calls upon the mafic tonalite-granodiorite parental magmas to exist with a refractory assemblage of 30 percent hornblende, 30 percent garnet, 40 percent clinopyroxene (that is, hornblende eclogite restite). Isotopic arguments will be presented in the following section to explain the 99.3 percent MORB to 0.7 percent deep sea sediment mix. A close fit exists between the average REE pattern of the six mafic tonalites-granodiorites and the model REE pattern (fig. 11), suggesting that the MORB partial melting model is appropriate.

Drummond and Defant (1990) and Defant and Drummond (1990) defined a set of geochemical parameters for magmas derived from a MORB source at amphibolite to eclogite facies conditions. Table 8 indicates that based on these parameters other trace element charateristics support a hornblende eclogite melting model for parental EQD generation. Y and Yb are found to have low concentrations in intermediate to felsic melts derived from the slab at garnet amphibolite–eclogite conditions because of their retention in refractory garnet. The inability of refractory plagioclase to survive eclogitic P-T conditions allows Sr to be enriched in a coexisting melt phase. A combination of restitic garnet and efficient removal of feldspar components from the slab upon melting provides the high Sr/Y and La/Yb ratios characteristic of slab melting.

Drummond and Defant (1990) demonstrated that high-Al tonalitic rocks generally have low K/Rb ratios (table 8) similar to the mafic EQD tonalites-granodiorites. They suggested that hornblende extraction either by restite control or fractionation could explain these low K/Rb ratios because of hornblende's greater affinity for K than for Rb (Arth and Hanson, 1975; Glikson, 1976). As shown in figure 9, K/Rb actually increases with differentiation, suggesting that the initial low K/Rb in the EQD is either inherited from the source or due to residual hornblende. For example, if a source of 99.3 percent altered MORB + 0.7 percent subducted sediment component (K/Rb = 62.5 and 600, respectively; McCulloch and Gamble, 1991) is assumed for the EQD, then the source K/Rb would equal 66. Figure 9 illustrates that K/Rb increases from 100 to 380 with differentiation. Assuming a linear mixing model, restite–source–parental magma–fractionated daughter magma should fall along a compositional curve with the source residing between the restite and parental magma compositions. Given these restrictions the estimated low K/Rb for this assumed source is consistent with the fact that the EQD's

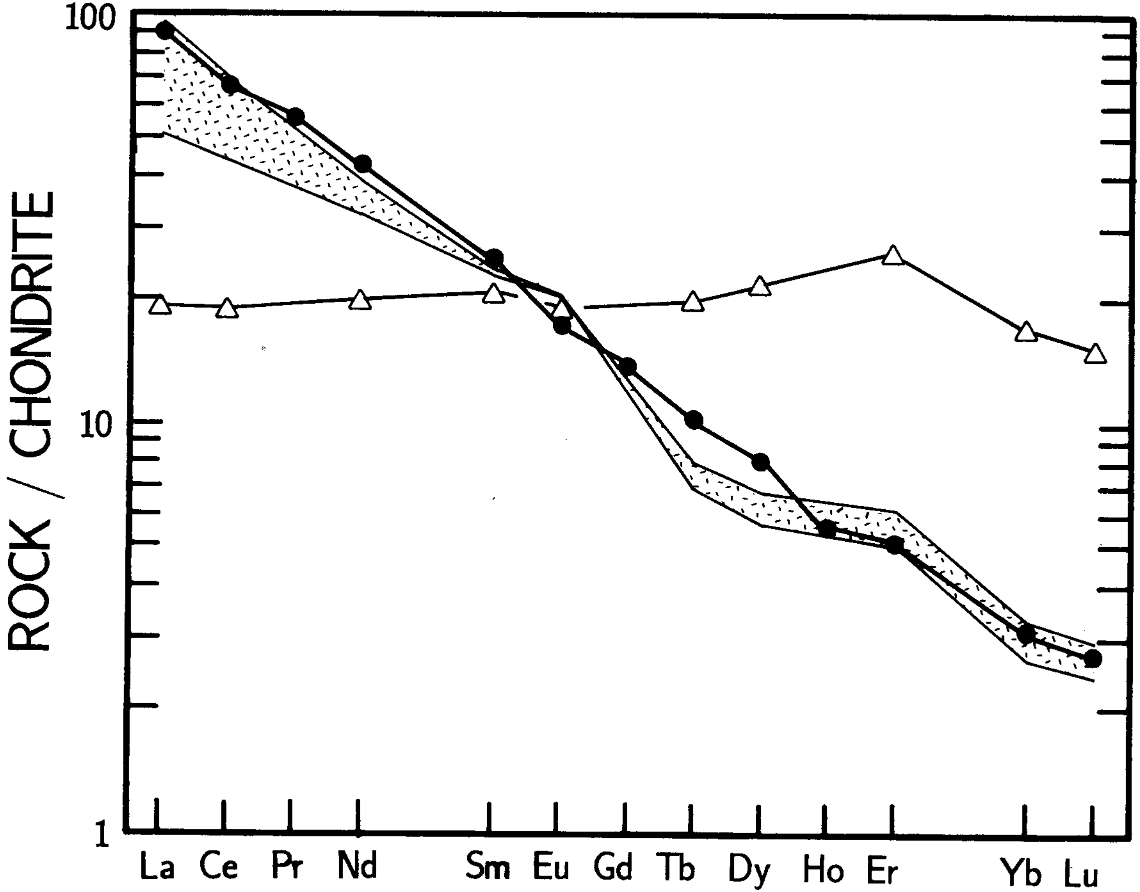

Fig. 11. A REE petrogenetic model for the tonalites-granodiorites of the EQD (closed circle pattern) indicates that 10 to 30 percent partial melting of a MORB + deep sea sediment source (99.3 percent MORB + 0.7 percent deep sea sediment; triangle pattern) under hornblende eclogite conditions (30 percent hornblende–30 percent garnet–40 percent clinopyroxene restite) produces a set of REE patterns (stippled region) that closely corresponds to the EQD data.

TABLE 8

Geochemical characteristics of felsic melts derived from a garnet amphibolite-eclogite slab source, parental EQD samples, and I-type granites

Parameter	Slab Melt*	EQD**	I-type Granite***
Al_2O_3 content at 70% SiO_2 level	> 15% Al_2O_3 at 70% SiO_2 level	15.9% Al_2O_3 at 70% SiO_2 level†	
Yb	< 1.9 ppm	0.70 ± 0.28 ppm	
Y	< 15 ppm	10.6 ± 2.5 ppm	27 ppm
Sr	> 600 ppm	642 ± 77 ppm	253 ppm
Sr/Y	> 40	62 ± 10	9.4
La/Yb	> 20	51 ± 22	
K/Rb	< 550	158 ± 24	192
Nb	< 10–11 ppm	7.4 ± 4.0 ppm	9 ppm

* Parameters defined by Drummond and Defant (1990) and Defant and Drummond (1990).

** An average of six mafic tonalites and granodiorites taken to represent parental EQD magma.

*** Average I-type granite composition from White and Chappell (1983).

† Determined from SiO_2 versus Al_2O_3 linear regression equation.

source should be < 100. The relatively high K/Rb for both the upper crust (K/Rb = 250) and lower crust (K/Rb) = 528) (Taylor and McLennan, 1985) argues against them as potential sources.

Lastly, the average Nb content in the six EQD mafic tonalites-granodiorites is less than the maximum value proposed for slab melt derivation (table 8). On a chondrite-normalized "spider" diagram (not shown) the assumed parental tonalite-granodiorite of the EQD displays a strong negative Nb anomaly relative to adjacent large ion lithophile elements (Ba and La). The low concentrations and negative anomaly of Nb are characteristic trace element signatures of modern calc-alkaline arc magmas. Niobium is thought to be depleted in the slab derived magmas by either the refractory nature and/or early crystallization of hornblende (Drummond and Defant, 1990).

Comparison of the average mafic tonalite-granodiorite of the EQD with average Australian I-type granite (White and Chappell, 1983) indicates a similarity in K/Rb and Nb contents that may be due to hornblende differentiation, as discussed above. However, the Australian I-types have relatively high Y and low Sr values because of their presumed lower continental crust derivation and attendant plagioclase-rich, garnet-poor nature of the restite. Thus, even though the EQD is I-type (that is, derived from an igneous source), it is distinct from the classic Australian I-type granite in the sense that it is not derived from the continental crust. This is an important distinction to make regarding the addition of new continental crustal material versus crustal recycling.

Isotopic modeling.—Oxygen isotopes provide signatures of the source of granitic magmas and the effects of open system processes. A preliminary study (Wesolowski, Drummond, and Gomolka, 1987) of the EQD's whole rock oxygen isotope compositions was accomplished on extremely fresh EQD samples which displayed no observable alteration, grain size denudation, or secondary mineralization on the microscopic scale. If this study is representative of the EQD, then the batholith has a narrow range of values, averaging 9.7 ± 0.4 permil (one sigma standard deviation of seven samples), which, in comparison to the primitive initial Sr value (0.7036), provides an isotopic engima. Normally, I-type granitoids of lower crustal origin have whole-rock values in the 6 to 8 permil range (Takahashi, Aramaki, and Ishihara, 1980). Interaction with metasediments could provide a mechanism for elevating $\delta^{28}O$ in the EQD. The average oxygen isotope and initial Sr isotope values for the host metasedimentary rocks are 12.2 permil (Drummond, Wesolowski, and Allison, 1988) and 0.715 (Russell, 1978), indicating that any mix between EQD magma and host metasediment should also elevate the EQD's initial Sr isotope value above its relatively low value. Furthermore, the constancy of $\delta^{18}O$ values in the EQD argues against any type of open system behavior, including assimilation and metasomatism (Drummond, Ragland, and Wesolowski, 1986). Chemical interaction between granitic rocks and metamorphic fluids has been documented in detail (Drummond, Ragland, and Wesolowski, 1986; Drummond, Wesolowski, and Allison, 1988) west of the EQD in the Rockford-type granitoids of the Rockford and Richville quadrangles (fig. 3). A wide range (7.6-14.1 permil) of oxygen isotope values were produced in the Rockford-type granitoids as a result of infiltration metasomatism. This type of metasomatic oxygen isotope signature is not observed in the EQD.

A model that explains this apparent incongruous isotopic behavior requires partial melting of a source with primitive Sr isotopic charater but elevated $\delta^{18}O$ values. The low initial Sr isotope ratio for the EQD indicates that the source was either mantle or mantle-derived basalt; a lower crustal metasedimentary or granulitic source is precluded by the low initial Sr ratio. The paucity of mafic material argues against the EQD being a fractionation product from a mantle-derived magma. A possible candidate is oceanic crust subjected to low temperature submarine alteration (producing elevated $\delta^{18}O$ values; Muehlenbachs, 1986). Table 1 provides the Sr isotopic data and simple mass balance calculations to indicate that the EQD's low initial Sr ratio of 0.7036 can be generated from a source composed of 99.3 percent altered MORB (93 percent MORB + 6.3 percent 500 Ma seawater) plus 0.7 percent deep sea sediment. The restrictions that can be placed on the proportions of each component are <7 percent H_2O in a submarine altered MORB (Humphris and Thompson, 1978) and <1 percent deep sea sediment (Hole and others, 1984). In addition, 99.3 percent altered MORB at 9.5 to 9.6 permil $\delta^{18}O$ (Muehlenbachs, 1986) and 0.7 percent deep sea sediment at 26 to 31 permil (Savin and Epstein, 1970; Yeh and Saving, 1976) are consistent with generating a granitic magma with 9.7 permil $\delta^{18}O$ by equilibrium partial melting. The exact proportions of the components used in the ternary mix may not be unique but demonstrate that mixing between these three components with restrictions on the H_2O and sediment content can provide the requisite O and Sr isotopic values.

Based on geochemical modeling and tectonic observations, Drummond and Defant (1990) and Defant and Drummond (1990) have demonstrated that partial melting of a subducting slab is facilitated in a tectonic regime where young (<20-30 Ma) oceanic crust is being subducted. Peacock (1990) found that subduction of young, hot oceanic crust is required for slab melting based on experimental petrology and numerical heat transfer models. These studies suggest that a mantle-derived MORB with a short crustal residence time (that is, young slab) could provide the necessary source for the EQD parental magmas.

TECTONIC IMPLICATIONS

The early Ordovician (490-500 Ma, table 1) age assigned the EQD is uncommon in terms of the magmatic-orogenic development of the Blue Ridge, because it: (1) post-dates synrift magmatism associated with the opening of the Iapetus Ocean (630 ± 60 Ma; Odom and Fullagar, 1984; Fichter and Diecchio, 1986); (2) predates all known plutonic episodes associated with the Taconic orogeny (440-470 Ma) of the Blue Ridge (Tull, 1980; Glover and others, 1983); and (3) predates prograde regional metamorphism (Acadian) and all other plutonic events in the Northern Alabama Piedmont (Thomas and others, 1980). All geologic periods, epochs, and ages stated in the following discussion are quoted relative to the DNAG geologic time scale (Palmer, 1983).

Tectonic models.—Two working hypotheses can be tested for the tectonic setting of the EQD:

1. Accreted terrane model (fig. 12A): During the Cambro-Ordovician, eastern North America (Laurentia) experienced stable platform carbonate deposition. Because concomitant carbonate deposition and continental margin magmatism are considered improbable in passive margin tectonic environments, the host terrane of the EQD may be exotic. This model supports the interpretations of Hatcher (1978), Cook and others (1979), and Hatcher and Odom (1980), who considered the eastern Blue Ridge and Inner Piedmont to be a tectonically active microcontinent or island arc during Early Cambrian to Early Ordovician time. Closure of a marginal basin between eastern North America and the microcontinent/island arc by eastward directed subduction would lead to accretion of the exotic terrane (Piedmont suspect terrane; Williams and Hatcher, 1982) and initiation of the Taconic orogeny.

Horton, Drake, and Rankin (1989) have refined the accreted terrane model for the southern and central Appalachians, subdividing the Piedmont terrane into the Jefferson and Inner Piedmont terranes. The Jefferson terrane stretches from the subsurface of Alabama to northern Virginia and in effect represents the eastern Blue Ridge. Lithologic units of the Jefferson terrane include parts of the Lynchburg, Catoctin, and Ashe Formations, Alligator Back and Tallulah Falls Formations, and Coweeta Group from the Carolinas and northern Georgia (Hatcher, 1979); Richard Russell Formation and the Helen, Sandy Springs, and New Georgia Groups of Georgia (Abrams and McConnell, 1981); and Wedowee Group and Ashland Supergroup (Tull, 1978) and Emuckfaw Formation (Neathery and Reynolds, 1975) of Alabama. Horton, Drake, and Rankin (1989) interpreted the Jefferson terrane as exotic, representing a metamorphosed accretionary wedge thrust onto Laurentia during the Taconic orogeny. They based this argument primarily on the presence of ultramafic rocks in the Jefferson terrane which they considered to be ophiolites.

2. Continental margin model (fig. 12B): In order to present this model one must first understand the timing of events recorded by rocks with known Laurentian affinities in the southern Appalachians during the Cambro-Ordovician. The easternmost rocks in Alabama accepted as Laurentian strata are those of the Talladega belt (Tull and others, 1988) (fig. 1). Rocks coeval with the EQD in the adjacent Talladega belt may include units in the upper part of the Sylacauga Marble Group. Tull (1985) and Tull and others (1988) stated that the top of the passive margin, miogeoclinal carbonates in the Talladega belt contains Early Ordovician (early to middle Arenigian, 485-488 Ma) conodonts. These units are overlain by a regional unconformity (pre-Lay Dam unconformity), which marks the transition from a passive to an active continental margin and closure of the Iapetus Ocean (Tull, 1984). The Lay Dam Formation overlies the unconformity and has been interpreted as a rapidly deposited diamictite during the Siluro-Devonian ($\sim$410 Ma) based on lithologic and fossil evidence (Tull and others, 1988; Tull and Telle, 1989). Thus, the pre-Lay Dam unconformity could document a long lived hiatus ($\sim$75 Ma) in the western Blue Ridge depositional record. Early or early Middle Ordovician (475-490 Ma) regional unconformities occur throughout the foreland of the Appalachians, marking the transition from a trailing margin to a convergent margin (Rodgers, 1983).

In the Alabama foreland, the post-Knox unconformity (Butts, 1926) is interpreted to represent this change in tectonic style and may accompany the peripheral bulge-flexural moat vertical displacements associated with carbonate shelf deformation during the late Early Ordovician ($\sim$485 Ma) in the Alabama Appalachians (Roberson, Benson, and Walker, 1988). Recent paleontological data on carbonates at Pratt Ferry, central Alabama (Shaw, Roberson, and Harris, 1990) tightly constrain the age of the post-Knox unconformity between 480 and 485 Ma. Drake and others (1989) have shown that the post-Knox unconformity in the southern Appalachians from Alabama to Virginia lasted from about 490 to 480 Ma. This implies that a relatively short lived ($\leq$10 Ma) unconformity was developed approx 480 to 485 my ago in the Alabama foreland.

The Middle Ordovician Blount wedge (Thomas, 1977) was developed in the foreland of southeast Tennessee and began with Athens Shale sedimentation in Alabama and Tennessee (table 9). The Middle Ordovician Blount clastic wedge material in the foreland requires an east to

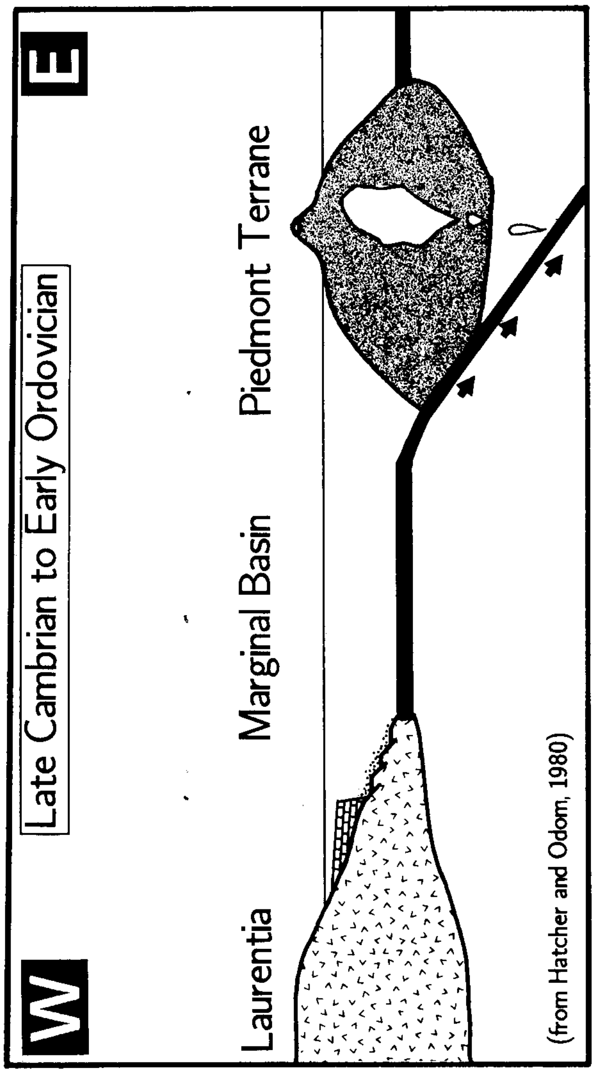

A.

Fig. 12(A) Tectonic schematic illustrating the accreted terrane model for the southern Appalachians during the Cambro-Ordovician and potential mode of EQD emplacement into an island arc/microcontinent setting.

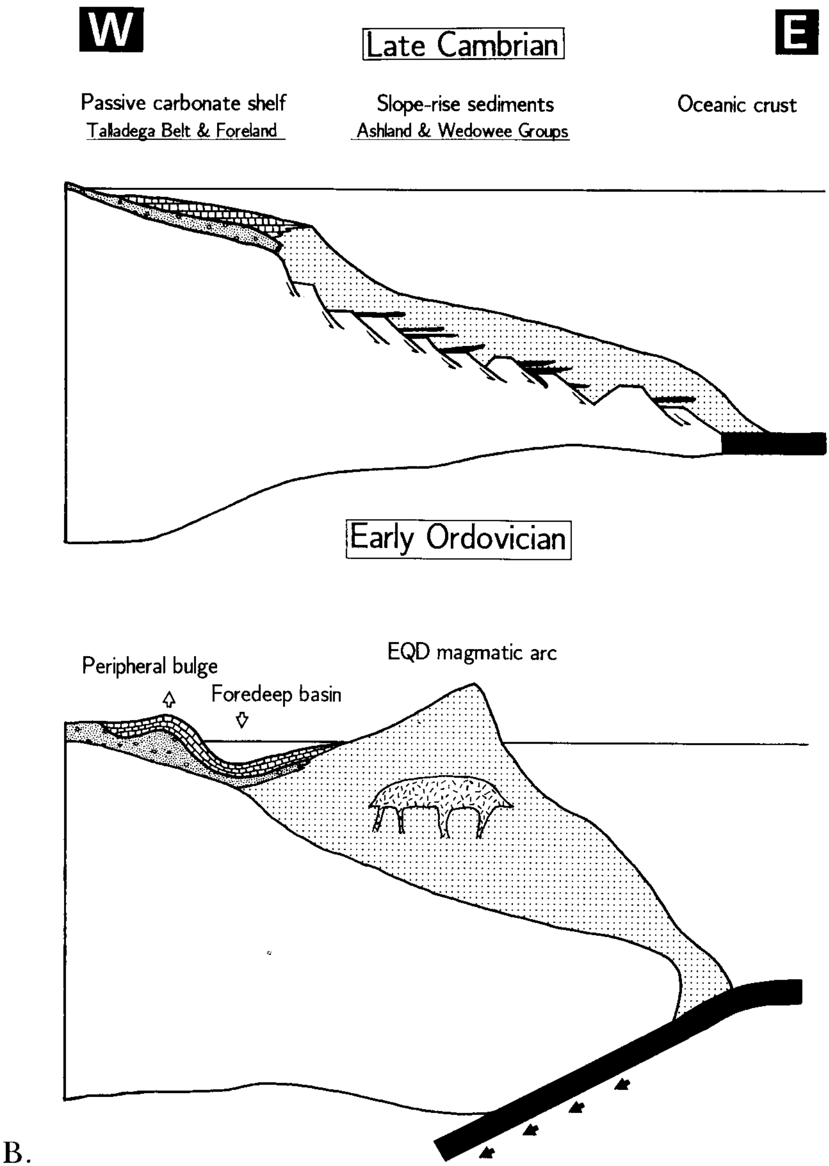

(B) Tectonic schematic illustrating the continential margin model for evolution of the Laurentian margin from a Late Cambrian passive margin to an Early Ordovician incipient collisional setting. Postulated relationship of the EQD and host rocks to proven Laurentian crustal material (Talledega Belt and Foreland stratigraphy) is shown.

TABLE 9

Significant Cambro-Ordovician events of the Alabama Appalachians

460 Ma	Zana and Kowaliga Granitic Gneiss emplacement (Russell, Odom, and Russell, 1987).
465 to 471 Ma	Collisional foredeep and drowning of shelf with carbonate to shale transition, as dated by graptolite zones in the Athens Shale of Alabama and Tennessee (*G. teretiusculus* zone, 464–466 Ma) and the Rockmart Slate of Georgia (*D. murchisoni,* 466–471 Ma) (Bradley, 1989).
480 to 485 Ma	Inception of the post-Knox regional unconformity during the late Canadian to early Whiterockian stages according to Mussman and Read (1986) and Shaw, Roberson, and Harris (1990).
485 to 490 Ma	Peripheral bulge-flexural moat pair records shelf deformation during the late Early Ordovician in the Alabama Appalachians (Roberson, Benson, and Walker, 1988).
490 to 500 Ma	Emplacement of the EQD granodiorite-tonalite batholith marking the Penobscot orogeny of the Alabama Appalachians.

southeast source (Drahovzal and Neathery, 1971; Thomas, 1977), which has been associated with uplift during late Early Ordovician to Late Ordovician Taconic thrusting (Rodgers, 1983). An additional source for the clastic wedge material could be provided by uplift associated with EQD magmatism at or near the continental margin. Read (1989) called upon initial subduction of the Iapetus Ocean and incipient collision of Laurentia during the Early Ordovician to convert the Late Cambrian shelf to an Early Ordovician ramp in the U.S. Appalachians. Therefore, regional unconformity and clastic wedge development in the Alabama Appalachian miogeocline may be a clear response to uplift and erosion associated with EQD continental margin magmatism.

Discussion

Horton, Drake, and Rankin's (1989) interpretation that the amphibolites and associated pyroxenites from the Ashland Supergroup represent ophiolitic fragments from a Taconic accretionary prism is their primary evidence for including the eastern Blue Ridge of Alabama into the suspect Jefferson terrane. However, Tull (1978), Thomas and others (1980), Stow, Neilson, and Neathery (1984), Drummond (ms), and Drummond, Wesolowski, and Allison (1988) consider these amphibolites to represent submarine volcanics associated with rifting of Laurentia based on their association with continental slope and rise sedimentary sequences and geochemical signature. Kline (1991) provides further objection to the Jefferson terrane on the basis of a detailed provenance study of Swift Run and Mechum River Formations, Lynchburg Group, and sandstone lenses in the Catoctin Formation of north Virginia. Meta-arkoses from these formations in northern Virginia contain blue quartz and perthite with a rod-like structure typical of granulite facies metamorphic terranes and were apparently derived from a proximal Grenville Blue Ridge basement source. Kline concludes that these metasedimentary units argue for a native Laurentian origin and that the Jefferson terrane is not suspect.

The timing of EQD intrusion coincides with the Penobscotian (520-485 Ma)–Grampian (520-490 Ma)–Finnmarkian (535-485 Ma) orogenies of the Appalachians, British and Scandinavian Caledonides, respectively (Harris and Fettes, 1988). Each of these orogenic events is associated with calc-alkaline magmatism, ophiolite obduction, and metamorphism (table 10). Many workers relate these pre-Taconic orogenic episodes to initial closure of the Iapetus Ocean either by continental margin subduction (Phillips, Stillman, and Murphy, 1976; Lambert and McKerrow, 1976; Williams, 1977; Sturt, Pringle, and Ramsay, 1978; Dewey and Shackleton, 1984; Wones and Sinha, 1988; Leake, 1989) or closure of marginal basins and terminating with island arc-continental margin collision (Jamieson, 1988; Dunning and Pederson, 1988; Rast, Sturt, and Harris, 1988; Skehan, 1988; Horton, Drake, and Rankin, 1989). The determination of whether orogenesis occurred on Laurentia or an offshore arc is a fundamental measure of subduction polarity during initial closure of the Iapetus Ocean. In fact, contemporaneous continent- and arc-directed subduction is documented in different parts of the Caledonide orogen during the Cambro-Ordovician. For example, Grampian metamorphic and magmatic events in western Ireland (table 10) are best explained by a north to northwest-dipping subduction zone beneath the southeast edge of Laurentia (Leake, 1989; Dewey and Ryan, 1990). On the other hand, the Penobscotian events in the Dunnage zone of Newfoundland (table 10) represent island arc magmatism and ophiolite obduction associated with the closure of a small marginal basin (O'Brien, O'Brien, and Dunning, 1991; Dunning and others, 1991). In other parts of the Appalachian-Caledonide mountain chain the character of the Cambro-Ordovician tectonic setting is more problematic.

Figure 13 illustrates the similar spatial relationship between the EQD, other potential Penobscot orogenic effects, the postulated Laurentian continental margin, and exotic arc terranes accreted to Laurentia during the Taconic orogeny. As shown in figure 13, the Penobscot-age igneous and metamorphic events in the southern and central Appalachians (table 10) closely coincide with the postulated eastern edge of the Laurentian margin and are located cratonward of adjacent accreted island arc terranes. This suggests that these magmatic-metamorphic episodes may be best explained by continental margin orogenesis rather than accreted terrane tectonics. In the southern Appalachians the accreted island-arc terrane is represented by the Carolina terrane (Whitney and others, 1978; Secor and others, 1983; Williams and Hatcher, 1982), which is interpreted to have accreted to Laurentia by Middle Ordovician time ($\sim$455 Ma) (Vick, Channell, and Opdyke, 1987; Dennis, 1988; Noel, Spariosu, and Dallmeyer, 1988). If the EQD was generated by continental margin magmatism, then a marginal basin would have separated Laurentia from the Carolina terrane during the Cambro-Ordovician.

TABLE 10

Cambro-Ordovician orogenic effects in the Appalachian-Caledonian mountain chain

I. Finnmarkian orogeny: Scandinavian Caledonides	
1. Nepheline syenite dike, Seiland Igneous Province, Norway; Sturt, Pringle, and Ramsay (1978)	501 ± 27 Ma Rb-Sr whole-rock
2. Finnmarkian slaty cleavage development northern Norway; Sturt, Pringle, and Ramsay (1978)	500–520 Ma Rb-Sr whole-rock
3. Seve eclogites, peak of metamorphism, Norrbotten, Sweden; Mork, Kullerud, and Stabel (1988)	503–505 Ma Sm-Nd mineral + whole-rock
4. Karmoy ophiolite, Norway; Dunning and Pederson (1988)	493 ± 7 Ma U-Pb zircon
5. Gullfjellet ophiolite, Norway; Dunning and Pederson (1988)	489 ± 3 Ma U-Pb zircon
6. Leka ophiolite, Norway; Dunning and Pederson (1988)	497 ± 2 Ma U-Pb zircon
7. Geitung Unit volcanics, southwest Norway; Dunning and others (1991)	495 ± 2 Ma U-Pb zircon
8. Tjopasi Group trondhjemite, Koli nappe, Sweden; Stephens and others (1985)	488 ± 5 Ma U-Pb zircon
9. Vallerlien trondhjemite, Norway; Stephens and others (1985)	509 ± 5 Ma U-Pb zircon
II. Grampian orogeny: Scottish and Irish Caledonides	
1. Slieve Gamph Complex granodiorite, Ox Mountains, northwest Ireland; Max, Long, and Sonet (1976)	500 ± 18 Ma Rb-Sr whole-rock
2. Connemara Gabbros, northwest Ireland; Jagger and others (1988)	490 ± 1 Ma U-Pb zircon
3. Connemara Schist, metamorphic peak, northwest Ireland; Leggo, Tanner, and Leake (1969)	510 ± 30 Ma Rb-Sr whole-rock
4. Ballantrae ophiolite, Scotland; Bluck and others (1980)	487 ± 8 Ma and 483 ± 4 Ma K-Ar whole-rock and U-Pb zircon
5. Dunfallandy Hill granite, Scotland; Pankhurst and Pidgeon (1976)	491 ± 15 Ma Rb-Sr whole-rock
6. Newer/Aberdeenshire Gabbros, Scotland; Pankhurst (1970)	490 ± 17 Ma Rb-Sr whole-rock
III. Penobscotian orogeny	
A. Newfoundland Appalachians	
1. Bay of Islands ophiolite complex, Humber terrane; Mattinson (1976)	504 ± 10 Ma U-Pb zircon
2. Little Port trondhjemite, Humber terrane; Dunning and Krogh (1986)	505 ± 3 Ma U-Pb zircon
3. Betts Cove ophiolite complex, Dunnage terrane; Dunning and Krough (1985)	489 ± 3 Ma U-Pb zircon
4. Pipestone Pond-Coy Pond ophiolite complex; Dunnage terrane; Dunning and Krough (1985)	494 ± 3 Ma U-Pb zircon
5. Twillingate trondhjemite, Dunnage terrane; Elliott, Dunning, and Williams (1991)	507 ± 3 Ma U-Pb zircon
6. Ernie Pond gabbro, Dunnage terrane; O'Brien, O'Brien, and Dunning (1991)	495 ± 2 Ma U-Pb zircon
7. Wild Cove granite, Dunnage terrane; O'Brien, O'Brien, and Dunning (1991)	499 ± 3 Ma U-Pb zircon
8. Tulks Hill metarhyolite, Dunnage terrane; Dunning and others (1991)	498 Ma U-Pb zircon

TABLE 10
(continued)

B. Northern Appalachians	
1. Penobscotian-type area, Maine-southeast Quebec	520–485 Ma
2. Blueschist metamorphism of mafic schist, northern Vermont; Laird (1988)	490–505 Ma 40Ar/39Ar (barroisite)
3. Cortlandt Complex, eastern New York; Ratcliffe and others (1982)	483 ± 10 and 496 ± 7 Ma K-Ar (hornblende)
4. Tetagouche Group granite, New Brunswick; Fyffe, Irrinki, and Cormier (1977)	489 ± 14 Ma Rb-Sr whole-rock
5. Thetford ophiolite obduction, southeast Quebec; Clague, Frankel, and Eaby (1985)	491 ± 3 Ma K-Ar whole-rock
C. Central Appalachians	
1. Arden plutton, Wilmington Complex, southeast Pennsylvania; Foland and Muessig (1978)	502 ± 20 Ma Rb-Sr whole-rock
2. Baltimore Gabbro, Maryland; Shaw and Wasserburg (1984)	490 ± 20 Ma Nd-Sm whole-rock
3. Port Deposit Complex, Maryland; Sinha, Hund, and Hogan (1989)	515 Ma U-Pb zircon
4. Occoquan batholith, northern Virginia; Mose and Nagel (1982)	494 ± 14 Ma Rb-Sr whole-rock
D. Southern Appalachians	
1. Southern Virginia Blue Ridge phyllites, metamorphic event; Fullagar and Dietrich (1976)	520 ± 19 Ma Rb-Sr whole-rock
2. Melrose pluton, Virginia Blue Ridge; Sinha, Hund, and Hogan (1989)	515 Ma U-Pb zircon
3. Leatherwood Granite, Virginia Blue Ridge; Sinha, Hund, and Hogan (1989)	516 Ma U-Pb zircon
4. Henderson Gneiss, North Carolina Inner Piedmont; recalculated from Odom and Fullagar (1973)	509 ± 27 Ma Rb-Sr whole-rock
5. Elkahatchee Quartz Diorite; Russell, Odom, Russell (1987)	490–500 Ma Rb-Sr whole-rock and U-Pb zircon

Given the above information, we favor the continental margin model for the EQD because: (1) continental margin orogenesis could provide the deformation required for the early Ordovician unconformities in both the Talladega belt and foreland of Alabama. The potential longevity of the pre-Lay Dam unconformity in the Talladega belt (≤ 75 Ma) versus the post-Knox unconformity in the foreland (≤ 10 Ma) may be a function of the more proximal nature of the Talladega belt to the proposed source for uplift (that is, Penobscot orogenesis associated with EQD genesis); (2) uplift associated with EQD magmatism at or near the continental margin could provide an additional east to southeast source (Drahovzal and Neathery, 1971; Thomas, 1977) for the Middle Ordovician clastic wedge material in the foreland; (3) continental margin plutonism is consistent with the intrusion of the EQD into continental margin slope-rise Wedowee Group sediments. If the EQD was emplaced into an island-arc setting, one would expect arc volcanics to comprise a major component of the host rock; and (4) continent-directed subduction of young marginal basin crust between Laurentia and the Carolina terrane is consistent with our

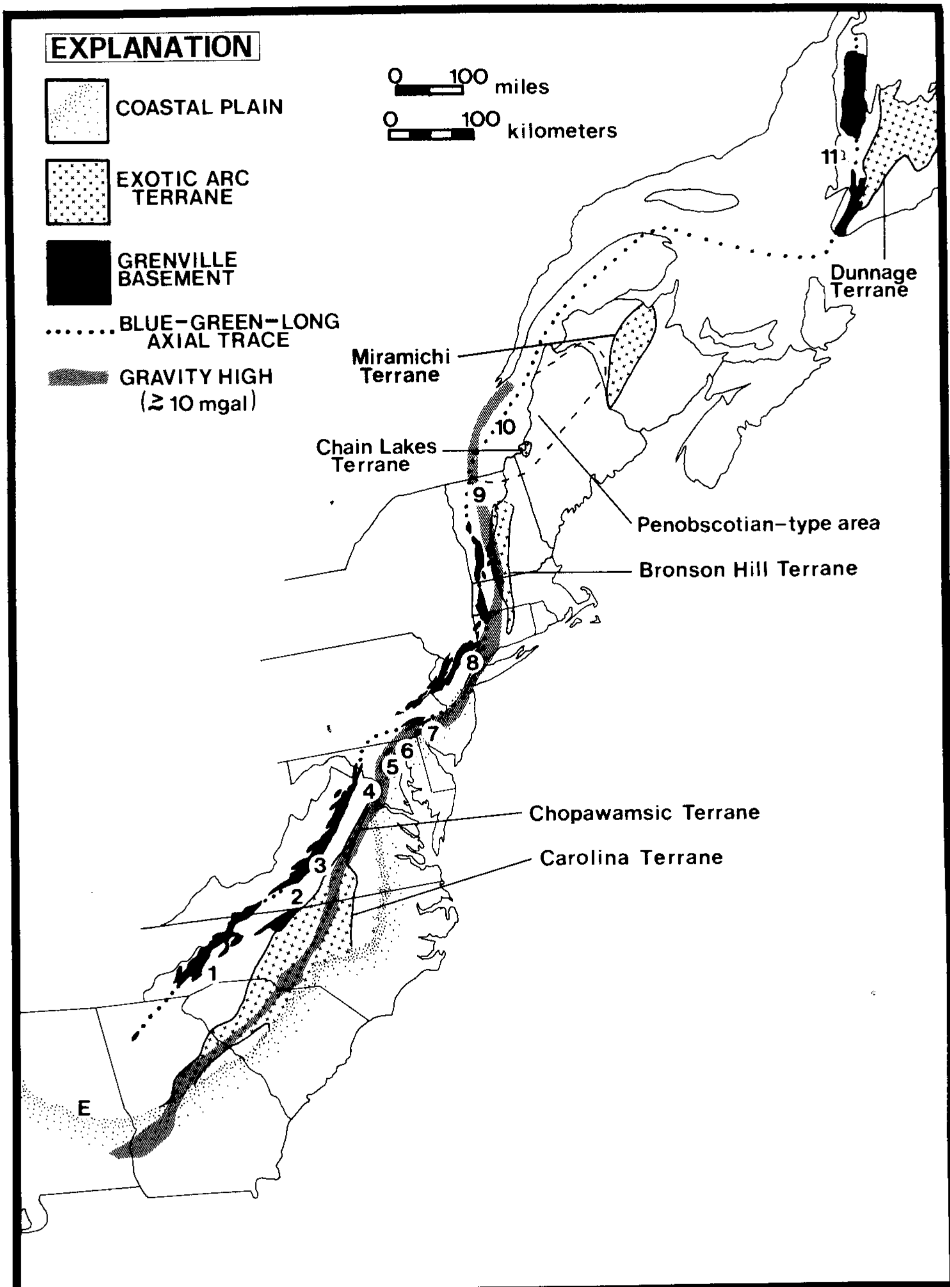
EXPLANATION
COASTAL PLAIN
EXOTIC ARC TERRANE
GRENVILLE BASEMENT
BLUE-GREEN-LONG AXIAL TRACE
GRAVITY HIGH (≳ 10 mgal)
0 100 miles
0 100 kilometers
Dunnage Terrane
Miramichi Terrane
Chain Lakes Terrane
Penobscotian-type area
Bronson Hill Terrane
Chopawamsic Terrane
Carolina Terrane
11
10
9
8
7
6
5
4
3
2
1
E

Figure 13

petrogenetic model interpreted for the EQD, that is, partial melting of young oceanic crust in a subduction zone setting. Thus, generation of the EQD is interpreted to mark the initiation of a Wilson cycle reversal in the southern Appalachian orogen.

Assuming a 495 Ma age for the EQD continental margin magmatism, 455 Ma time of Carolina terrane accretion to Laurentia, orthogonal closure between Laurentia and the Carolina terrane, and 4 cm/yr velocity of Ordovician plate motion in the Iapetus (as measured by Van der Voo and others, 1991), then the Early Ordovician separation of the eastern Laurentian margin from the Carolina terrane would be approx 1600 km. This distance is similar to the separation determined paleomagnetically between Laurentia's western Newfoundland margin and the Dunnage terrane ($\sim$ 1500 km) by Van der Voo and others (1991).

Sinha, Hund, and Hogan (1989) suggested that the plutonic rocks defining the Penobscot-age magmatic event in the central and southern Appalachians (table 10) may record continental arc development. Detailed lithologic and geochemical studies of the Baltimore mafic complex (table 10) (Shaw and Wasserburg, 1984; Hanan and Sinha, 1989) indicate an ensialic origin for the complex as the roots of a continental arc volcanic complex or as a marginal basin developed inland of a continental margin arc complex. Contrary to the statement of Horton, Drake, and Rankin (1989) that "Evidence of a Penobscotian orogeny has not been found south of Virginia . . . ," we present evidence for Penobscotian orogenic effects in the southern Appalachians. This study and that of Hanan and Sinha (1989) provide detailed information on the two largest, Penobscotian felsic and mafic plutonic bodies in the central and southern Appalachians with each study consistently interpreting a continental margin origin.

When using the term "Penobscot orogeny" in this paper we refer to a specific time of Appalachian orogenesis and not a specific method of mountain building. In fact, Boone and Boudette (1989) have suggested that Late Cambrian to Early Ordovician mountain building in the type Penobscot area (fig. 13) is the result of collision between two exotic island arcs (Boundary Mountain and Gander terranes) in the Iapetus and not continental margin orogenesis as interpreted here for the EQD. The

Fig. 13. Relationship of the study area (E) to the suggested eastern edge of the Laurentian continental margin (Blue-Green-Long axis: Rankin, 1975; eastern North America gravity high: Cook and Oliver, 1981), exotic island-arc terranes accreted to Laurentia during the Late Cambrian to Late Ordovician (Carolina terrane, see text; Chopawamsic terrane, Pavlides, 1985; Bronson Hill terrane, Robinson and Hall, 1980; Chain Lakes terrane, Rast, Sturt, and Harris, 1988; Miramichi terrane, Van Staal, 1987; Dunnage terrane, Williams and Hatcher, 1982), and other potential Penobscotian-age orogenic effects (numbered 1–11). Refer to table 10 for additional information on the below listed Cambro-Ordovician orogenic events. (1) Henderson Gneiss, (2) southern Virginia phyllites and Leatherwood Granite, (3) Melrose pluton, (4) Occoquan batholith, (5) Baltimore Gabbro, (6) Port Deposit Complex, (7) Arden pluton, (8) Cortlandt Complex, (9) blueschist metamorphism, Vermont, (10) Thetford ophiolites, (11) Bay of Islands ophiolite and Penobscotian-type area (Skehan, 1988).

Boundary Mountain terrane is areally expansive, encompassing the Chain Lakes terrane, the Penobscot-type area, the northwest extremity of the Bronson Hill terrane, and borders the northwest side of the Miramichi terrane (fig. 13). A continuous link of exotic island arc terranes is produced by the Bronson Hill terrane (Robinson and Hall, 1980; Leo, 1985), Boundary Mountain terrane (Boone and Boudette, 1989), Miramichi terrane (Whitehead and Goodfellow, 1978; van Staal, 1987; van Staal, Winchester, and Bedard, 1991), and Dunnage zone (Payne and Strong, 1979; Dunning and others, 1991) from Connecticut to Newfoundland which Williams and Hatcher (1982) collectively termed the Dunnage terrane. These findings are in contrast to the EQD and other events numbered on figure 13 that may represent Penobscot-age orogenesis on the Laurentian margin. Thus, Penobscot orogenic events may have affected both the continental margin and offshore island arcs, and only through detailed analyses can one determine the tectonic style for a specific Penobscot orogenic event. For example, a recent study by Trzcienski, Rodgers, and Guidotti (1992) on the Chain Lakes terrane casts doubt on its exotic terrane status. They suggest that the Chains Lake terrane may represent a diamictite unit proximal to North America during the Penobscot orogeny.

SUMMARY

A combination of mineralogic and geochemical observations suggests that the EQD parental magmas were derived by partial melting of altered MORB source material under hornblende eclogite metamorphic conditions. Magma production is interpreted to be associated with continental margin orogenesis and subduction of young, back arc basin oceanic crust which separated Laurentia from the Carolina arc terrane. We propose that the EQD magmas may have ascended through the Laurentian continental crust in an extensional tectonic regime like that documented for the Peruvian Coastal batholith (Pitcher, 1978). Initial magmatic ascent could be provided by fractures and final emplacement by roof uplift and block stoping. Detailed field studies, structural analyses, and downplunge tectonic reconstructions suggest that the final intrusive form of the EQD was laccolithic with a concordant roof grading at depth into discordant feeder dikes. All the physical observations made on the EQD are consistent with the feeder dike–inflated sill–roof doming emplacement stages for laccoliths (Corry, 1988).

Upon ascent, dynamic sidewall crystallization occurred within the EQD magma chamber with initial crystallization of andesine–hornblende–biotite–Fe-epidote–apatite at a temperature and pressure of 790° to 850°C and 3 to 4 kb, respectively. This early crystallization assemblage aggregated as cumulate gabbroic to dioritic layers (?) or lenses along the outer periphery of the EQD magma chamber but were severely dismembered into meter- to centimeter-size enclaves by magmatic convection (fig. 6). The early fractionation assemblage differentiated the granitic melt toward more felsic varieties of tonalite and granodiorite. Disrupted hornblende-biotite gabbro-diorite enclaves were allowed to mix and react convectively with the evolving EQD melt phase, recrystallizing them into the biotite-epidote schistose enclaves found scattered throughout the main mass (tonalite-granodiorite) of the EQD. A later crystallization assemblage of andesine–quartz–biotite–K-feldspar–hornblende allowed the tonalite-granodiorite to evolve to the felsic EQD endmembers (trondhjemite and granite). These felsic granitoids are present in the central portion of the EQD batholith and result from dynamic crystallization toward the batholithic core. Few enclaves reside within the felsic granitoids, possibly due to the low temperatures and crystal-rich character of the EQD magma at this late stage, creating high viscosities and negligible flow.

The presence of cogenetic metadacite porphyry located along the laccolith's upper cupola suggests that the EQD batholith was subvolcanic and responsible for dacitic volcanics in a continental margin tectonic setting. Intrusion of the EQD into its own volcanic ejecta ceased its vertical ascent due to reaching a neutrally buoyant elevation in the crust. Final emplacement as an inflated sill produced the resultant laccolithic intrusive form.

We suggest that the EQD may play a pivotal role in refining the orogenic history of the Appalachians. The model presented here suggests that the EQD represents the magmatic response of the Laurentian margin to incipient subduction and closure of the Iapetus Ocean. Other Early Ordovician plutons in the central and southern Appalachians (table 10 and fig. 13) may also record the initiation of subduction and closely mark the Cambro-Ordovician Laurentian margin. We propose that the Penobscotian orogeny may have been a widespread tectonic event associated with continental margin orogenesis (table 10, fig. 13) and represents the birth of the long-lived Appalachian mountain building event. The importance of the Penobscotian event may have been overlooked in the past, because superposition of the Taconic, Acadian, and Alleghenian dynamothermal episodes has probably obscured any structural and/or metamorphic effect associated with the Penobscot orogeny. Rare exceptions to this include the metamorphic ages from the southern Virginia Blue Ridge phyllites and northern Vermont blueschists (table 10). Specific plutons (table 10) are the only lithologic vestiges of Penobscotian orogenic effects in the southern and central Appalachians. It is only through a diversity of detailed field, structural, mineralogic, and geochemical studies that one can construct a reasonable model for a complex batholithic body such as the EQD. In this case, the EQD's geologic and petrogenetic model sheds some light on a key stage in the history of the Appalachians.

ACKNOWLEDGMENTS

Acknowledgment is made to the Donors of The Petroleum Research Fund, administered by the American Chemical Society, for the support of this research. The senior author would like to acknowledge Florida State

University's Chevron Foundation for the initial support of this research. DJW's effort was supported by the Geoscience Program of the United States Department of Energy, Office of Basic Energy Sciences, under contract DE-AC-05-84OR21400 with Martin Marietta Systems, Inc. The expert advice on microprobe operation by Mike Bersch, University of Alabama, is appreciated. Comments on the initial manuscript were provided by Denny Bearce, Mike Neilson, and Jim Tull. Many thanks to Barry Gilliam of Alabama Power Company for allowing us to sample core material. Journal reviews provided by Bob Hatcher, Calvin Miller, and Robert Tracy are gratefully acknowledged. It is our hopes that this research will be as helpful to future geologists as H. R. Gault's study fifty years ago on the EQD was to us.

APPENDIX

Whole-rock geochemical accuracy and precision estimates

Accuracy*/Precision** Estimate		
SiO_2 = 0.36/0.2	B = 2.4/14	La = 0.88/0.46
TiO_2 = 2.8/0	Ba = 2.7/2.5	Ce = 0.25/3.7
Al_2O_3 = 1.4/0	Be = 4.2/1.5	Pr = 7.7/3.4
$Fe_2O_3^*$ = 2.4/1.5	Co = 4.5/1.9	Nd = 2.0/1.5
MnO = 4.3/0	Cr = 3.2/20	Sm = 1.5/1.2
MgO = 3.1/0	Cu = 1.9/11	Eu = 8.2/3.9
CaO = 1.2/0.4	Li = 7.5/0	Gd = 0/1.7
Na_2O = 0.93/1.0	Nb = 9.1/0	Tb = 4.2/0
K_2O = 2.6/1.1	Ni = 7.1/16	Dy = 0.3/3.9
P_2O_5 = 14.5/0	Rb = 2.0/0	Ho = 3.9/3.8
	Sc = 13.1/1.8	Er = 1.1/5.5
	Sr = 7.2/0	Tm = 0/0
	Ta = 6.25/0	Yb = 2.4/2.5
	Th = 5.4/4.0	Lu = 4.9/2.4
	U = 2.2/0	
	V = 8.4/2.4	
	Y = 10.0/0	
	Zn = 0/0.9	
	Zr = 2.6/1.8	

* percent deviation = [(accepted-obtained)100]/accepted.
** percent coefficient of variation = 100(standard deviation/mean).

REFERENCES

Abrams, C. E., and McConnell, K. I., 1981, Stratigraphy of the area around the Austell-Frolona antiform: West-central Georgia: Georgia Geological Survey, Information Circular 54-A, p. 55–67.

Allison, D. T., ms, 1992, Structural development and petrogenesis of a granite-metasediment complex, Coosa County, Alabama: Ph.D. thesis, Florida State University, Tallahassee, 444 p.

Arth, J. G., and Hanson, G. N. 1975, Geochemistry and origin of the early Precambrian crust of northeastern Minnesota: Geochimica et Cosmochimica Acta, v. 39, p. 325–362.

Barbarin, B., 1990, Granitoids: main petrogenetic classifications in relation to origin and tectonic setting: Geochemical Journal, v. 25, p. 227–238.

Barker, F., 1979, Trondhjemite: definition, environment and hypotheses of origin, *in* Barker, F., editor, Trondhjemites, Dacites, and Related Rocks: New York, Elsevier, p. 1–12.

Barker, F., Arth, J. G., Peterman, Z. E., and Friedman, I., 1976, The 1.7- to 1.8-b.y.-old trondhjemites of southwestern Colorado and northern New Mexico: Geological Society of America Bulletin, v. 87, p. 189–198.
Barth, A. P., 1990, Mid-crustal emplacement of Mesozoic plutons, San Gariel Mountains, California, and implications for the geologic history of the San Gabriel terrane, *in* Anderson, J. L., editor, The Nature and Origin of Cordilleran Magmatism: Geological Society of America Memoir 174, p. 33–45.
Bence, A. E., and Albee, A. L., 1968, Empirical correction fractions for the electron microanalysis of silicates and oxides: Journal of Geology, v. 76, p. 382–403.
Bluck, B. J., Halliday, A. N., Aftalion, M., and Macintyre, R. M., 1980, Age and origin of Ballantrae ophiolite and its significance to the Caledonian orogeny and Ordovician time scale: Geology, v. 8, p. 492–495.
Blundy, J. D., and Holland, T. J. B., 1990, Calcic amphibole equilibria and a new amphibole-plagioclase geothermometer: Contributions to Mineralogy and Petrology, v. 104, p. 208–224.
Boone, G. M., and Boudette, E. L., 1989, Accretion of the Boundary Mountains terrane within the northern Appalachian orthotectonic zone, *in* Horton, J. W., Jr., and Rast, N., editors, Melanges and Olistostromes of the U.S. Appalachians: Geological Society of America Special Paper 228, p. 17–42.
Bradley, D. C., 1989, Taconic plate kinematics as revealed by foredeep stratigraphy, Appalachian orogen: Tectonics, v. 8, p. 1037–1049.
Brophy, J. G., and Marsh, B. D., 1986, On the origin of high-alumina arc basalt and the mechanics of melt extraction: Journal of Petrology, v. 27, p. 763–787.
Burnham, C. W., 1979, Magmas and hydrothermal fluids, *in* Barnes, H. L. editor, Geochemistry of Hydrothermal Ore Deposits: New York, John Wiley, p. 71–136.
Bussell, M. A., and Pitcher, W. S., 1985, The structural controls of batholith emplacement, *in* Pitcher, W. S. and others, editors, Magmatism at a Plate Edge—The Peruvian Andes: London, Blackie, p. 167–176.
Butts, C., 1926, The Paleozoic rocks, *in* Adams, G. I. and others, Geology of Alabama: Tuscaloosa, Alabama, Geological Survey of Alabama, Special Report 14, p. 40–223.
Castro, A., Moreno-Ventas, I., and de la Rosa, J. D., 1990, Microgranular enclaves as indicators of hybridization processes in granitoid rocks, Hercynian Belt, Spain: Geochemical Journal, v. 25, p. 391–404.
Chen, Y. D., Price, R. C., White, A. J. R., and Chappell, B. W., 1990, Mafic inclusions from the Glenborg and Blue Gum granite suites, southeastern Australia: Journal of Geophysical Research, v. 95, p. 17,757–17,785.
Clague, D. A., Frankel, C. S., and Eaby, J. S., 1985, The age and origin of felsic intrusions of the Thetford Mines ophiolite, Quebec: Canadian Journal of Earth Science, v. 22, p. 1257–1261.
Cook, F. A., Albaugh, O. S., Brown, L. D., Kaufman, S., Oliver, J. E., and Hatcher, R. D., 1979, Thin-skinned tectonics in the crystalline southern Appalachians; COCORP seismic-reflection profiling of the Blue Ridge and Piedmont: Geology, v. 7, p. 563–567.
Cook, F. A., and Oliver, J. E., 1981, The late Precambrian-early Paleozoic continental edge in the Appalachian orogen: American Journal of Science, v. 281, p. 993–1008.
Corry, C. E., 1988, Laccoliths; Mechanics of Emplacement and Growth: Geological Society of America Special Paper 220, 120 p.
Crawford, J. L., and Russell, G. S., 1989, Strontium initial ratios and Rb-Sr mineral ages from an Elkahatchee Quartz Diorite/trondhjemite pluton contact, Alexander City, Tallapoosa County, Alabama: Geological Society of America, Abstracts with Programs, v. 21, p. 10.
Deer, W. A., Howie, R. A., and Zussman, J., 1982, An Introduction to the Rock-Forming Minerals, 13th edition: Essex, England, Longman, 528 p.
Defant, M. J., and Drummond, M. S., 1990, Derivation of some modern arc magmas by melting of young subducted lithosphere: Nature, v. 347, p. 662–665.
Dennis, A., 1988, Preliminary report on the geology of the Glenn Springs—Jonesville area and tectonic model, *in* Secor, D. T., editor, Southeastern Geological Excursions: Columbia, South Carolina, South Carolina Geological Survey, p. 226–239.
Dewey, J. F., and Ryan, P. D., 1990, The Ordovician evolution of the South Mayo Trough, western Ireland: Tectonics, v. 9, p. 887–901.
Dewey, J. F., and Shackleton, R. M., 1984, A model for the evolution of the Grampian tract in the early Caledonides and Appalachians: Nature, v. 312, p. 115–121.
Didier, J., and Barbarin, B., editors, 1991, Enclaves and Granite Petrology: New York, Elsevier, 625 p.

Dodge, F. C. W., and Kistler, R. W., 1990, Some additional observations on inclusions in the granitic rocks of the Sierra Nevada: Journal of Geophysical Research, v. 95, p. 17,841–17,848.

Drahovzal, J. A., and Neathery, T. L., 1971, Middle and Upper Ordovician stratigraphy of the Alabama Appalachians, *in* Drahovzal, J. A., and Neathery, T. L., editors, The Middle and Upper Ordovician of the Alabama Appalachians: Alabama Geological Society, v. 9, p. 1–62.

Drake, A. A., Jr., Sinha, A. K., Laird, J., and Guy, R. E., 1989, The Taconic orogen, *in* Hatcher, R. D., Thomas, W. A., and Viele, G. W., editors, The Appalachian—Ouachita Orogen in the United States: Boulder, Colorado, Geological Society of America, v. F-2, p. 101–177.

Drummond, M. S., ms, 1986, Igneous, metamorphic and structural history of the Alabama Tin Belt, Coosa County, Alabama: Ph.D. thesis, Florida State University, Tallahassee, 411 p.

——— 1987, Rockford Granite, Coosa County, Alabama: I. Geologic setting, occurrence, petrography and mineral chemistry, *in* Drummond, M. S., and Green, N. L., editors, Granites of Alabama: Tuscaloosa, Alabama, Geological Survey of Alabama, Special Publication, p. 117–130.

Drummond, M. S., and Defant, M. J., 1990, A model for trondhjemite–tonalite–dacite genesis and crustal growth via slab melting: Archean to modern comparisons: Journal of Geophysical Research, v. 95, p. 21,503–21,521.

Drummond, M. S., Ragland, P. C., and Wesolowski, D., 1986, An example of trondhjemite genesis by means of alkali metasomatism, Rockford Granite, Alabama Appalachians: Contributions to Mineralogy and Petrology, v. 93, p. 98–113.

Drummond, M. S., Wesolowski, D., and Allison, D. T., 1988, Generation, diversification, and emplacement of the Rockford Granite, Alabama Appalachians: Mineralogic, petrologic, isotopic (C & O), and P-T constraints: Journal of Petrology, v. 29, p. 869–897.

Dunning, G. R., and Krogh, T. E., 1985, Geochronology of ophiolites of the Newfoundland Appalachians: Canadian Journal of Earth Sciences, v. 22, p. 1659–1670.

——— 1986, Geochronology of ophiolites of the Newfoundland Appalachians: a reply: Canadian Journal of Earth Sciences, v. 23, p. 1862–1864.

Dunning, G. R., and Pederson, R. B., 1988, U/Pb ages of ophiolites and arc-related plutons of the Norwegian Caledonides: implications for the development of Iapetus: Contributions to Mineralogy and Petrology, v. 98, p. 13–23.

Dunning, G. R., Swinden, H. S., Kean, B. F., Evans, D. T. W., and Jenner, G. A., 1991, A Cambrian island arc in Iapetus: geochronology and geochemistry of the Lake Ambrose volcanic belt, Newfoundland Appalachians: Geological Magazine, v. 128, p. 1–17.

Elliott, C. G., Dunning, G. R., and Williams, P. F., 1991, New U/Pb zircon age constaints on the timing of deformation in north-central Newfoundland and implications for early Paleozoic Appalachian orogenesis: Geological Society of America Bulletin, v. 103, p. 125–135.

Evans, B. W., and Vance, J. A., 1987, Epidote phenocrysts in dacitic dikes, Boulder County, Colorado: Contributions to Mineralogy and Petrology, v. 96, p. 178–185.

Faure, G., 1986, Principles of Isotope Geology: New York, John Wiley, 589 p.

Fichter, L. S., and Diecchio, R. J., 1986, Stratigraphic model for timing of the opening of the proto-Atlantic Ocean in northern Virginia: Geology, v. 14, p. 307–309.

Flood, R. H., and Shaw, S. E., 1979, K-rich cumulate diorite at the base of a tilted granodiorite pluton from the New England Batholith, Australia: Journal of Geology, v. 87, p. 417–425.

Foland, K. A., and Muessig, K. W., 1978, A Paleozoic age for some charnockitic-anorthositic rocks: Geology, v. 6, p. 143–146.

Fullagar, P. D., and Dietrich, R. V., 1976, Rb-Sr isotopic study of the Lynchburg and probably correlative formations of the Blue Ridge and western Piedmont of Virginia and North Carolina: American Journal of Science, v. 276, p. 347–365.

Fyffe, L. R., Irrinki, R. R., and Cormier, R. F., 1977, A radiometric age of deformed granitic rocks in north-central New Brunswick: Canadian Journal of Earth Sciences, v. 14, p. 1687–1689.

Gault, H. R., 1945, Petrography, structures, and petrofabrics of the Pinckneyville Quartz Diorite, Alabama: Geological Society of America Bulletin, v. 56, p. 181–246.

Geist, D. J., Baker, B. H., and McBirney, A. R., 1985, GPP: A Program Package for Creating and Using Geochemical Data Files: Eugene, Oregon, University of Oregon, 33 p.

Gill, J. B., 1981, Orogenic Andesites and Plate Tectonics: New York, Springer-Verlag, 390 p.
Glickson, A. Y., 1976, Trace element geochemistry and origin of early Precambrian acid igneous series, Barberton Mountain Land, Transvaal: Geochimica et Cosmochimica Acta, v. 40, p. 1261–1280.
Glover, L., Speer, J. A., Russell, G. S., and Farrar, S. S., 1983, Ages of regional metamorphism and ductile deformation in the central and southern Appalachians: Lithos, v. 16, p. 223–245.
Gromet, L. P., and Silver, L. T., 1983, Rare earth element distributions among minerals in a granodiorite and their petrogenetic implications: Geochimica et Cosmochimica. Acta, v. 47, p. 925–939.
Gunow, A. J., Ludington, S., and Munoz, J. L., 1980, Fluorine in micas from the Henderson Molybdenite Deposit, Colorado: Economic Geology, v. 75, p. 1127–1131.
Hamilton, W., and Myers, W. B., 1974, Nature of the Boulder Batholith of Montana: Geological Society of America Bulletin, v. 85, p. 365–378.
Hammarstrom, J. M., and Zen, E-An, 1986, Aluminum in hornblende: an empirical igneous geobarometer: American Mineralogist, v. 71, p. 1297–1313.
Hanan, B. B., and Sinha, A. K., 1989, Petrology and tectonic affinity of the Baltimore mafic complex, Maryland, *in* Mittwede, S. K., and Stoddard, E. F., editors, Ultramafic Rocks of the Appalachian Piedmont: Geological Society of America Special Paper 231, p. 1–18.
Hanson, G. N., 1978, The application of trace elements to the petrogenesis of igneous rocks of granitic composition: Earth and Planetary Science Letters, v. 38, p. 26–43.
Harris, A. L., and Fettes, D. J., editors, 1988, The Caledonian-Appalachian Orogen: Oxford, England, Blackwell Scientific, 643 p.
Harris, N. B. W., Pearce, J. A., and Tindle, A. G., 1986, Geochemical characteristics of collision-zone magmatism, *in* Coward, M. P., and Ries, A. C., editors, Collision Tectonics: Oxford, England, Blackwell Scientific, p. 67–81.
Hatcher, R. D., 1978, Tectonics of the western Piedmont and Blue Ridge, southern Appalachians: review and speculation: American Journal of Science, v. 278, p. 276–304.
———— 1979, The Coweeta Group and Coweeta syncline: Major features of the North Carolina-Georgia Blue Ridge: Southeastern Geology, v. 21, p. 17–29.
Hatcher, R. D., and Odom, A. L., 1980, Timing of thrusting in the southern Appalachians, USA: model for orogeny?: Journal of the Geological Society (London), v. 137, p. 321–327.
Henderson, P., 1982, Inorganic Geochemistry: New York, Pergamon, 353 p.
Hole, M. J., Saunders, A. D., Marriner, G. F., and Tarney, J., 1984, Subduction of pelagic sediments: implications for the origin of Ce-anomalous basalts from the Mariana Islands: Journal of the Geological Society (London), v. 141, p. 453–472.
Horton, J. W., Drake, A. A., and Rankin, D. W., 1989, Tectonostratigraphic terranes and their Paleozoic boundaries in the central and southern Appalachians, *in* Dallmeyer, R. D., editor, Terranes in the Circum-Atlantic Paleozoic Orogens: Geological Society of America Special Paper 230, p. 213–245.
Humphris, S. E., and Thompson, G., 1978, Hydrothermal alteration of oceanic basalts by seawater: Geochimica et Cosmochimica Acta, v. 42, p. 107–125.
Jagger, M. D., Max, M. D., Aftalion, M., and Leake, B. E., 1988, U-Pb zircon ages of basic rocks and gneisses intruded into the Dalradian rocks of Cashel, Connemara, western Ireland: Journal of the Geological Society (London), v. 145, p. 645–648.
Jamieson, R. A., 1988, Metamorphic P-T-t data from western Newfoundland and Cape Breton—implications for Taconian and Acadian tectonics: Geological Association of Canada, Abstracts with Programs, v. 13, p. A60.
Johnson, M. C., and Rutherford, M. J., 1989, Experimental calibration of the aluminum-in-hornblende geobarometer with application to Long Valley caldera (California) volcanic rocks: Geology, v. 17, p. 837–841.
Kline, S. W., 1991, Provenance of arkosic metasediments in the Virginia Blue Ridge: constraints on Appalachian suspect terrane models: American Journal of Science, v. 291, p. 189–198.
Laird, J., 1988, Arenig to Wenlock age metamorphism in the Appalachians, *in* Harris, A. L., and Fettes, D. J., editors, The Caledonian-Appalachian Orogen: Oxford, England, Blackwell Scientific, p. 311–345.
Lambert, R. S. J., and McKerrow, W. S., 1976, The Grampian orogeny: Scottish Journal of Geology, v. 12, p. 271–292.

Leake, B. E., 1971, On aluminous and edenitic hornblendes: Mineralogical Magazine, v. 38, p. 389–407.

———— 1978, Nomenclature of amphiboles: Mineralogical Magazine, v. 42, p. 533–563.

———— 1989, The metagabbros, orthogneisses and paragneisses of the Connemara complex, western Ireland: Journal of the Geological Society (London), v. 146, p. 575–596.

Leggo, P. J., Tanner, P. W. G., and Leake, B. E., 1969, Isochron study of Donegal granite and certain Dalradian rocks of Great Britian, *in* Kay, M., editor, North Atlantic—Geology and Continental Drift, A Symposium: American Association of Petroleum Geologists, Memoir 12, p. 354–362.

Leo, G. W., 1985, Trondhjemite and metamorphosed quartz keratophyre tuff of the Ammonoosuc (Ordovician), western New Hampshire and adjacent Vermont and Massachusetts: Geological Society of America Bulletin, v. 96, p. 1493–1507.

London, D., Cerny, P., Loomis, J. L., and Pan, J. J., 1990, Phosphorus in alkali feldspars of rare-element granitic pegmatites: Canadian Mineralogist, v. 28, p. 771–786.

Marshall, B. D., and DePaolo, D. J., 1989, Calcium isotopes in igneous rocks and the origin of granite: Geochimica et Cosmochimica Acta, v. 53, p. 917–922.

Mason, G. H., 1985, The mineralogy and textures of the Coastal Batholith, Peru, *in* Pitcher, W. S. and others, editors, Magmatism at a Plate Edge—The Peruvian Andes: London, Blackie, p. 156–166.

Mattinson, J. M., 1976, Ages of zircons from the Bay of Islands ophiolite complex, western Newfoundland: Geology, v. 4, p. 393–394.

Max, M. D., Long, C. B., and Sonet, J., 1976, The geological setting and age of the Ox Mountains Granodiorite: Geological Survey of Ireland Bulletin, v. 2, p. 27–35.

McCulloch, M. T., and Gamble, J. A., 1991, Geochemical and geodynamical constraints on subduction zone magmatism: Earth and Planetary Science Letters, v. 102, p. 358–374.

Miller, C. F., and Mittlefehldt, D. W., 1982, Depletion of light rare-earth elements in felsic magmas: Geology, v. 10, p. 129–133.

Miller, C. F., Watson, E. B., and Rapp, R. P., 1985, Experimental investigation of mafic mineral-felsic liquid equilibria: preliminary results and petrogenetic implications: EOS, v. 66, p. 1130.

Moore, W. B., Tull, J. F., and Allison, D. T., 1987, Intrusive chronology, progressive deformation, geochemistry of granitoid dikes and strain analysis of xenoliths, Northern Piedmont, Tallapoosa County, Alabama, *in* Drummond, M. S., and Green, N. L., editors, Granites of Alabama: Tuscaloosa, Alabama, Geological Survey of Alabama, Special Publication, p. 33–55.

Mork, M. B. E., Kullerud, K., and Stabel, A., 1988, Sm-Nd dating of Seve eclogites, Norrbotten, Sweden—evidence for early Caledonian (505 Ma) subduction: Contributions to Mineralogy and Petrology, v. 99, p. 344–351.

Mose, D. G., and Nagel, M. S., 1982, Plutonic events in the Piedmont of Virginia: Southeastern Geology, v. 23, p. 25–39.

Muecke, G. K., Pride, C., and Sarkar, P., 1977, Rare-earth element geochemistry of regional metamorphic rocks, *in* Ahrens, L. H., editor, Origin and Distribution of the Elements, volume II: New York, Pergamon, p. 449–464.

Muehlenbachs, K., 1986, Alteration of the oceanic crust and the ^{18}O history of seawater, *in* Valley, J. W., Taylor, H. P., Jr., and O'Neill, J. R., editors, Stable Isotopes in High Temperature Geological Processes: Reviews in Mineralogy, v. 16, p. 425–444.

Mussman, W. J., and Read, J. F., 1986, Sedimentology and development of a passive-to convergent margin unconformity: Middle Ordovician Knox unconformity, Virginia Appalachians: Geological Society of America Bulletin, v. 97, p. 282–295.

Naney, M. T., 1983, Phase equilibria of rock-forming ferromagnesian silicates in granitic systems: American Journal of Science, v. 283, p. 993–1033.

Neathery, T. L., and Reynolds, J. W., 1975, Geology of the Lineville East, Ofelia, Wadley North, and Mellow Valley quadrangles, Alabama: Geological Survey of Alabama Bulletin 109, 120 p.

Noel, J. R., Spariosu, D. J., and Dallmeyer, R. D., 1988, Paleomagnetism and $^{40}Ar/^{39}Ar$ from the Carolina slate belt, Albemarle, North Carolina: Implications for terrane amalgamation with North America: Geology, v. 16, p. 64–68.

O'Brien, B. H., O'Brien, S. J., and Dunning, G. R., 1991, Silurian cover, Late Precambrian–Early Ordovician basement, and the chronology of Silurian orogenesis in the Hermitage Flexure (Newfoundland Appalachians): American Journal of Science, v. 291, p. 760–799.

Odom, A. L., and Fullagar, P. D., 1973, Geochronologic and tectonic relationships between the Inner Piedmont, Brevard zone, and Blue Ridge belts, North Carolina: American Journal of Science, v. 273-A, p. 133–149.

——— 1984, The timing of opening of the Iapetus Ocean: Rb-Sr whole-rock and inherited zircon ages of the plutonic suite of the Crossnore Complex, southern Appalachians, and their implications regarding the time of opening of the Iapetus Ocean, *in* Bartholomew, M. J., editor, The Grenville Front in the Appalachians and Related Topics: Geological Society of America Special Paper 194, p. 255–261.

Palmer, A. R., 1983, The Decade of North American Geology 1983 geologic time scale: Geology, v. 11, p. 503–504.

Pankhurst, R. J., 1970, The geochronology of the basic igneous complexes: Scottish Journal of Geology, v. 6, p. 83–107.

Pankhurst, R. J., and Pidgeon, R. T., 1976, Inherited isotope systems and the source region pre-history of early Caledonian granites in the Dalradian Series of Scotland: Earth and Planetary Science Letters, v. 31, p. 55–68.

Paterson, S. R., Vernon, R. H., and Fowler, T. K., Jr., 1991, Aureole tectonics, *in* Kerrick, D. M., editor, Contact Metamorphism: Reviews in Mineralogy, v. 26, p. 673–722.

Pavlides, L., 1985, Early Paleozoic composite melange in the central Appalachian Piedmont, Virginia and Maryland: Geological Society of America, Abstracts with Programs, v. 17, p. 686.

Payne, J. G., and Strong, D. F., 1979, Origin of the Twillingate trondhjemite, north-central Newfoundland: Partial melting in the roots of an island arc, *in* Barker, F., editor, Trondhjemites, Tonalites, and Related Rocks: New York, Elsevier, p. 489–516.

Peacock, S. M., 1990, Numerical simulation of metamorphic pressure-temperature-time paths and fluid production in subducting slabs: Tectonics, v. 9, p. 1197–1211.

Pearce, J. A., Harris, N. B. W., and Tindle, A. G., 1984, Trace element discrimination diagrams for the tectonic interpretation of granitic rocks: Journal of Petrology, v. 25, p. 956–983.

Phillips, W. F. A., Stillman, C. J., and Murphy, T., 1976, A Caledonian plate tectonic model: Journal of the Geological Society (London), v. 132, p. 579–609.

Philpotts, J. A., and Schnetzler, C. C., 1970, Phenocryst-matrix partition coefficients for K, Rb, Sr and Ba with applications to anorthosite and basalt genesis: Geochimica et Cosmochimica Acta, v. 34, p. 307–322.

Pitcher, W. S., 1978, The anatomy of a batholith: Journal of the Geological Society (London), v. 135, p. 157–182.

——— 1983, Granite type and tectonic environment, *in* Hsu, K. editor, Mountain Building Processes: London, Academic Press, p. 19–40.

——— 1987, Granites and yet more granites: Geologische Rundschau, v. 76, p. 51–79.

Ramsay, J. G., 1967, Folding and Fracturing of Rocks: New York, McGraw-Hill, 568 p.

Rankin, D. W., 1975, The continental margin of eastern North America in the southern Appalachians: the opening and closing of the proto-Atlantic Ocean: American Journal of Science, v. 275-A, p. 298–336.

Rapp, R. P., Watson, E. B., and Miller, C. F., 1991, Partial melting of amphibolite/eclogite and the origin of Archean trondhjemites and tonalites: Precambrian Research, v. 51, p. 1–25.

Rast, N., Sturt, B. A., and Harris, A. L., 1988, Early deformation in the Caledonian-Appalachian orogen, *in* Harris, A. L., and Fettes, D. J., editors, The Caledonian-Appalachian Orogen: Oxford, England, Blackwell Scientific, p. 111–122.

Ratcliffe, N. M., Armstrong, R. L., Mose, D. G., Seneschal, R., Williams, N., and Baiamonte, M. J., 1982, Emplacement history and tectonic significance of the Cortlandt Complex, related plutons, and dike swarms in the Taconide zone of southeastern New York based on K-Ar and Rb-Sr investigations: American Journal of Science, v. 282, p. 358–390.

Read, J. R., 1989, Controls on evolution of Cambro-Ordovician passive margin, U. S. Appalachians, *in* Crevello, P. D. and others, editors, Controls on Carbonate Platform and Basin Development: Tulsa, Oklahoma, Society of Economic Paleontologists Mineralogists Special Publication 44, p. 147–165.

Roberson, K. E., Benson, D. J., and Walker, K. R., 1988, Stratigraphic evidence for late Early Ordovician shelf deformation in the Alabama Appalachians: Geological Society of America, Abstracts with Programs, v. 20, p. 311.

Robinson, P., and Hall, L. M., 1980, Tectonic significance of southern New England, *in* Wones, D. R., editor, The Caledonides of the USA: Blacksburg, Virginia, Virginia Institute of Technology, State University, Memoir 2, p. 73–82.

Rock, N. M. S., 1990, The International Mineralogical Association (IMA/CNMMN) pyroxene nomenclature scheme: computerization and its consequences: Mineralogy and Petrology, v. 43, p. 99–119.
Rodgers, John, 1983, The life history of a mountain range—the Appalachians, *in* Hsu, K., editor, Mountain Building Processes: London, Academic Press, p. 229–241.
Rushmer, T., Holloway, J. R., and Wyborn, D., 1985, Melting relations in a classic Australian I-type dacite at 10 kbars: EOS, v. 66, p. 1130.
Russell, G. S., 1975, Geochronologic investigations in the northern Alabama Piedmont, *in* Neathery, T. L., and Tull, J. F., editors, Geologic Profiles of the Northern Alabama Piedmont: Alabama Geologic Society Guidebook, v. 13, p. 87–98.
———— ms, 1978, U-Pb, Rb-Sr, and K-Ar isotopic studies bearing on the tectonic development of the southernmost Appalachian orogen, Alabama: Ph.D. thesis, Florida State University, Tallahassee, 196 p.
Russell, G. S., Odom, A. L., and Russell, C. W., 1987, Uranium-lead and rubidium-strontium isotopic evidence for the age and origin of granitic rocks in the Northern Alabama Piedmont, *in* Drummond, M. S., and Green, N. L., editors, Granites of Alabama: Tuscaloosa, Alabama, Geological Survey of Alabama, Special Publication, p. 239–249.
Sanders, C. O., 1984, Location and configuration of magma bodies beneath Long Valley, California, determined from anomalous signals: Journal of Geophysical Research, v. 89, p. 8287–8302.
Savin, S. M., and Epstein, S., 1970, The oxygen and hydrogen isotope geochemistry of ocean sediments and shales: Geochimica et Cosmochimica Acta, v. 34, p. 43–63.
Secor, D. T., Samson, D. L., Snoke, A. W., and Palmer, A. R., 1983, Confirmation of the Carolina Slate Belt as an exotic terrane: Science, v. 221, p. 649–651.
Shaw, D. R., 1972, The origin of the Apsley gneiss, Ontario: Canadian Journal of Earth Sciences, v. 5, p. 561–583.
Shaw, H. F., and Wasserburg, G. J., 1984, Isotopic constraints on the origin of Appalachian mafic complexes: American Journal of Science, v. 284, p. 319–349.
Shaw, T. H., Roberson, K. E., and Harris, A. G., 1990, Lithostratigraphy and conodont biostratigraphy across the lower-Middle Ordovician disconformity (Early to Middle Whiterockian) at Pratt Ferry, central Alabama: U.S. Geological Survey Bulletin 1895, p. C1–C13.
Shimokawa, T., Masuda, A., and Izawa, K., 1972, Rare earth elements in the top samples of the cores from the Pacific ocean floor: Geochemical Journal, v. 6, p. 75–81.
Sinha, A. K., Hund, E. A., and Hogan, J. P., 1989, Paleozoic accretionary history of the North American plate margin (central and southern Appalachians): constraints from the age, origin, and distribution of granitic rocks, *in* Hillhouse, J. W., editor, Deep Structure and Past Kinematics of Accreted Terranes: Washington, D.C., American Geophysical Union, Geophysical Monograph 50, p. 219–238.
Skehan, J. W., 1988, Evolution of the Iapetus Ocean and its borders in pre-Arenig times: a synthesis, *in* Harris, A. L., and Fettes, D. J., editors, The Caledonian-Appalachian Orogen: Oxford, England, Blackwell Scientific, p. 185–229.
Stephens, M. B., Furnes, H., Robins, B., and Sturt, B. A., 1985, Igneous activity within the Scandinavian Caledonides, *in* Gee, D. G., and Sturt, B. A., editors, The Caledonide Orogen—Scandinavia and Related Areas: New York, John Wiley and Sons, p. 953–978.
Stow, S. H., Neilson, M. J., and Neathery, T. L., 1984, Petrography, geochemistry, and tectonic significance of the amphibolites of the Alabama Piedmont: American Journal of Science, v. 284, p. 416–436.
Sturt, B. A., Pringle, I. R., and Ramsay, D. M., 1978, The Finnmarkian phase of the Caledonian orogeny: Journal of the Geological Society (London), v. 135, p. 597–610.
Takahashi, M., Aramaki, S., and Ishihara, S., 1980, Magnetite-series/ilmenite-series vs. I-type/S-type granitoids: Mining Geology Special Issue, no. 8, p. 13–28.
Taylor, S. R., and McLennan, S. M., 1985, The Continental Crust: Its Composition and Evolution: Oxford, England, Blackwell Scientific, 312 p.
Thomas, W. A., 1977, Evolution of Appalachian—Ouachita salients and recesses from reentrants and promontories in the continental margin: American Journal of Science, v. 277, p. 1233–1278.
Thomas, W. A., and Neathery, T. L., 1980, Tectonic framework of the Appalachian orogeny in Alabama, *in* Frey, R. W., editor, Excursions in Southeastern Geology: Alexandria, Virginia, American Geological Institute, p. 465–526.

Thomas, W. A., Tull, J. F., Bearce, D. N., Russell, G., and Odom, A. L., 1980, Geologic synthesis of the southernmost Appalachians, Alabama and Georgia, *in* Wones, D. R., editor, The Caledonides of the USA: Blacksburg, Virginia, Virginia Tech, Memoir 2, p. 91–97.

Trzcienski, W. E., Jr., Rodgers, J., and Guidotti, C. V., 1992, Alternative hypotheses for the Chain Lakes "massif," Maine and Quebec: American Journal of Science, v. 292, p. 508–532.

Tull, J. F., 1978, Structural development of the Alabama Piedmont northwest of the Brevard Zone: American Journal of Science, v. 278, p. 442–460.

——— 1980, Overview of the sequence and timing of deformational events in the southern Appalachians: evidence from the crystalline rocks, North Carolina to Alabama, *in* Wones, D. R., editor, The Caledonides of the USA: Blacksburg, Virginia, Virginia Institute of Technology and State University, Memoir 2, p. 167–178.

——— 1984, Polyphase late Paleozoic deformation in the southeastern foreland and northwestern Piedmont of the Alabama Appalachians: Journal of Structural Geology, v. 6, p. 223–234.

——— 1985, Stratigraphy of the Sylacauga Marble Group, *in* Tull, J. F., Bearce, D. N., and Guthrie, G. M., editors, Early Evolution of the Appalachian Miogeocline: Upper Precambrian—Lower Paleozoic Stratigraphy of the Talladega Slate Belt: Alabama Geological Society Guidebook, v. 22, p. 21–26.

——— 1987, Structural setting of granitic plutonism in the northern Piedmont, Alabama Appalachians, *in* Drummond, M. S., and Green, N. L., editors, Granites of Alabama: Tuscaloosa, Alabama, Geological Survey of Alabama, Special Publication, p. 17–31.

Tull, J. F., and Telle, W. R., 1989, Tectonic setting of olistostromal units and associated rocks in the Talladega slate belt, Alabama Appalachians, *in* Horton, J. W., Jr., and Rast, N., editors, Melanges and Olistostromes of the U.S. Appalachians: Geological Society of America Special Paper 228, p. 247–269.

Tull, J. F., Harris, A. G., Repetski, J. E., McKinney, F. K., Garrett, C. B., and Bearce, D. N., 1988, New paleontologic evidence constraining the age and paleotectonic setting of the Talladega slate belt, southern Appalachians: Geological Society of America Bulletin, v. 100, p. 1291–1299.

Trzcienski, W. E., Jr., Rodgers, J., and Guidotti, C. V., 1992, Alternative hypotheses for the Chain Lakes "massif," Maine and Quebec: American Journal of Science, v. 292, p. 508–532.

Van der Voo, R., Johnson, R. J. E., Van der Pluijm, B. A., and Knutson, L. C., 1991, Paleogeography of some vestiges of Iapetus: Paleomagnetism of the Ordovician Robert's Arm, Summerford, and Chanceport Groups, central Newfoundland: Geological Society of America Bulletin, v. 103, p. 1564–1575.

van Staal, C. R., 1987, Tectonic setting of the Tetagouche Group in northern New Brunswick: implications for plate tectonic models of the northern Appalachians: Canadian Journal of Earth Sciences, v. 24, p. 1329–1351.

van Staal, C. R., Winchester, J. A., and Bedard, J. H., 1991, Geochemical variations in Middle Ordovician volcanic rocks of the northern Miramichi Highlands and their tectonic significance: Canadian Journal of Earth Sciences, v. 28, p. 1031–1049.

Vernon, R. H., 1990, Crystallization and hybridism in microgranitoid enclave magmas: microstructural evidence: Journal of Geophysical Research, v. 95, p. 17,849–17,859.

Vick, H. K., Channell, J. E. T., and Opdyke, N. D., 1987, Ordovician docking of the Carolina Slate Belt: Paleomagnetic data: Tectonics, v. 6, p. 573–583.

Vyhnal, C., McSween, H. Y., Jr., and Speer, J. A. 1991, Hornblende chemistry in southern Appalachian granitoids: Implications for aluminium hornblende thermobarometry and magmatic epidote stability: American Mineralogist, v. 76, p. 176–188.

Wakita, H., Rey, P., and Schmitt, R. A., 1971, Abundances of the 14 rare-earth elements and 12 other trace elements in Apollo 12 samples: five igneous and one breccia rocks and four soils: Lunar Science Conference, 2d, Proceedings, p. 1319–1329.

Wampler, J. M., Neathery, T. L., and Bentley, R. D., 1970, Age relations in the Alabama Piedmont, *in* Bentley, R. D., and Neathery, T. L., editors, Geology of the Brevard Fault Zone: Alabama Geological Society Guidebook, v. 8, p. 81–90.

Watson, E. B., and Harrison, T. M., 1984, Accessory minerals and the geochemical evolution of crustal magmatic systems: a summary and prospectus of experimental approaches: Physics of the Earth and Planetary Interiors, v. 35, p. 19–30.

Wesolowski, D., Drummond, M. S., and Gomolka, J., 1987, Oxygen and carbon isotope distributions in granitoids and metasediments of the Rockford District and adjacent portions of the Northern Alabama Piedmont and Inner Piedmont, *in* Drummond, M. S., and Green, N. L., editors, Granites of Alabama: Tuscaloosa, Alabama, Geological Survey of Alabama, Special Publication, p. 221–238.
White, A. J. R., and Chappell, B. W., 1983, Granitoid types and their distributions in the Lachlan Fold Belt, southeastern Australia, *in* Roddick, J. A., editor, Circum-Pacific Plutonic Terranes: Geological Society of America Memoir 159, p. 21–34.
Whitehead, R. E., and Goodfellow, W. D., 1978, Geochemistry of volcanic rocks from the Tetagouche Group, Bathurst, New Brunswick, Canada: Canadian Journal of Earth Sciences, v. 15, p. 207–219.
Whitney, J. A., Paris, T. A., Carpenter, R. H., and Hartley, M. E., 1978, Volcanic evolution of the southern slate belt of Georgia and South Carolina: A primitive oceanic island arc: Journal of Geology, v. 86, p. 173–192.
Williams, H., 1977, Ophiolitic melange and its significance in the Fleur de Lys Supergroup, northern Appalachians: Canadian Journal of Earth Science, v. 14, p. 987–1003.
Williams, H., and Hatcher, R. D., 1982, Suspect terranes and accretionary history of the Appalachian orogen: Geology, v. 10, p. 530–536.
Wones, D. R., and Sinha, A. K., 1988, A brief review of early Ordovician to Devonian plutonism in the North American Caledonides, *in* Harris, A. L., and Fettes, D. J., editors, The Caledonian-Appalachian Orogen: Oxford, England, Blackwell Scientific, p. 381–388.
Woodhead, J. D., 1988, The origin of geochemical variations in Mariana lavas: A general model for petrogenesis in intraoceanic island arcs?: Journal of Petrology, v. 29, p. 805–830.
Wright, T. L., and Doherty, P. C., 1970, A linear programming and least squares computer method for solving petrologic mixing problems: Geological Society of America Bulletin, v. 81, p. 1995–2008.
Wyborn, D., Turner, B. S., and Chappell, B. W., 1987, The Boggy Plain Supersuite: a distinction belt of I-type igneous rocks of potential economic significance in the Lachlan Fold Belt: Australian Journal of Earth Science, v. 34, p. 21–43.
Yeh, H. W., and Savin, S. M., 1976, The extent of oxygen isotope exchange between clay minerals and sea water: Geochimica et Cosmochimica Acta, v. 42, p. 140–143.
Zen, E-An, and Hammarstrom, J. M., 1984, Magmatic epidote and its petrologic significance: Geology, v. 12, p. 515–518.